



**European Commission
Research Programme of the Research Fund for Coal and Steel**

INNOSEIS

Valorization of innovative anti-seismic devices

WORK PACKAGE 2 – DELIVERABLE 2.2

Validation of q-factors for innovative devices

Coordinator:

National Technical University of Athens - NTUA, Greece

Beneficiaries:

Universitatea Politehnica Timisoara - UPT, Romania

Politecnico di Milano - POLIMI, Italy

Universita Degli Studi di Napoli Federico II - UNINA, Italy

Universita di Pisa - UNIPI, Italy

Rheinisch-Westfaelische Technische Hochschule Aachen - RWTH, Germany

Instituto Superior Tecnico - IST, Portugal

Universitet po Arhitektura Stroitelstvo i Geodezija - UACEG, Bulgaria

Universiteit Hasselt - UHasselt, Belgium

Maurer Sohne Engineering GmbH & CO KG - MSE, Germany

Convention Europeenne de la Construction Metallique ASBL - ECCS, Belgium

Grant Agreement Number: 709434

30/09/2017

AUTHORS:

NATIONAL TECHNICAL UNIVERSITY OF ATHENS

Institute of Steel Structures

15780 Athens, Greece

Authors: Konstantinos Bakalis, Dimitrios Vamvatsikos, Stella Avgerinou, Panagiotis Tsarpalis, Pavlos Thanopoulos, Ioannis Vayas

POLITECNICO DI MILANO

Department of Architecture, Built Environment and Construction Engineering

Piazza Leonardo da Vinci, 32, 20133 Milan, Italy

Authors: Carlo Castiglioni, Alper Kanyilmaz, Amin Alavi, Giovanni Brambilla, Gianpaolo Chiarelli

UNIVERSITA DEGLI STUDI DI NAPOLI “FEDERICO II”

Department of Structures for Engineering and Architecture

Via Forno Vecchio 36, Napoli, 80134, Italy

Authors: Mario D’ Aniello, Raffaele Landolfo

UNIVERSITEIT HASSELT

Faculty of Engineering Technology

Agoralaan, Gebouw H, Diepenbeek 3590, Belgium

Authors: Jose Henriques, Hervé Degee

RHEINISCH-WESTFAELISCHE TECHNISCHE HOCHSCHULE AACHEN

Institute of Steel Construction

Mies-van-der-Rohe Str. 1, 52074 Aachen

Authors: Benno Hoffmeister, Marius Pinkawa

UNIVERSITA DI PISA

Department of Civil and Industrial Engineering,

Largo Lucio Lazzarino 1, 56122, Pisa, Italy

Authors: Francesco Morelli, Andrea Piscini, Walter Salvatore

POLITEHNICA UNIVERSITY OF TIMISOARA

Department of Steel Structures and Structural Mechanics

Ioan Curea Street, no.1, Timisoara, Romania

Authors: Calin Neagu, Adriana Chesoa, Aurel Stratan, Florea Dinu, Dan Dubina

INSTITUTO SUPERIOR TECNICO

Department of Civil Engineering, Architecture and Georesources

Av. Rovisco Pais, 1049-001 Lisbon, Portugal

Authors: Luís Calado, Jorge M. Proença, João Sio

UNIVERSITET PO ARCHITEKTURA STROITELSTVO I GEODEZIJA

Department of Steel and Timber Structures

1 Hr. Smirnski blvd. 1046 Sofia, Bulgaria

Authors: Lora Raycheva, Tzvetan Georgiev, Dimo Zhelev, Nikolaj Rangelov

TABLE OF CONTENTS

1	Introduction	1
2	INERD pin links	2
2.1	Modelling	2
2.2	Static Pushover Analysis	2
2.3	Incremental Dynamic Analysis	4
2.4	q-factor verification.....	4
3	INERD U links	5
3.1	Modelling	5
3.2	Static Pushover Analysis	5
4	FUSEIS beam links.....	6
4.1	Modelling	6
4.2	Static Pushover Analysis	6
4.3	Incremental Dynamic Analysis	8
4.4	q-factor verification.....	8
5	FUSEIS pin links.....	9
5.1	Modelling	9
5.2	Static Pushover Analysis	10
5.3	Incremental Dynamic Analysis	11
5.4	q-factor verification.....	12
6	FUSEIS bolted cover plate links	13
6.1	Modelling	13
6.2	Static Pushover Analysis	14
6.3	Incremental Dynamic Analysis	16
6.4	q-factor verification.....	17
7	FUSEIS welded cover plate links	18
7.1	Modelling	18
7.2	Static Pushover Analysis	20
7.3	Incremental Dynamic Analysis	22
7.4	q-factor verification.....	23
8	DUAREM removable link devices	24
8.1	Modelling	24
8.2	Static Pushover Analysis	24
8.3	Incremental Dynamic Analysis	26
8.4	q-factor verification.....	27
9	SPSW thin-walled steel panels	28
9.1	Modelling	28
9.2	Static Pushover Analysis	29
9.3	Incremental Dynamic Analysis	31
9.4	q-factor verification.....	31
10	CBF-MB Centrally-braced frames with modified sections	32

10.1 Modelling	32
10.2 Static Pushover Analysis	32
10.3 Incremental Dynamic Analysis	34
10.4 q-factor verification.....	34
11 Concluding remarks.....	35
References	36
List of Figures.....	37
List of Tables	39

1 Introduction

Within the INNOSEIS project, Vamvatsikos et al. [1] proposed a behaviour factor evaluation approach based on the explicit performance assessment of archetype structures using multiple performance targets on a mean annual frequency of exceedance basis. It comprises seven discrete steps:

1. Select sites, estimate the hazard and select ground motions
2. Define and design archetype buildings for a trial q-factor
3. Develop accurate nonlinear models
4. Perform preliminary evaluation via nonlinear static pushover analysis
5. Perform nonlinear dynamic analysis
6. Define performance criteria and estimate fragility curves
7. Accept or reject the trial q-factor

Normally, a normative application of the methodology requires a large sample of archetype buildings and one or more iterations until an optimal q-factor is reached. Herein, the proposed approach will be employed for the pre-normative assessment of 9 innovative steel lateral-load resisting systems, developed in European and National projects by the authors. For reasons of simplicity, only two to three archetype buildings will be employed. Uncertainty dispersions of $\beta_{LSU} = 0.2$ and $\beta_{GCU} = 0.3$ are assumed, together with a moderate confidence level of $x = 80\%$. Only a single pass will be undertaken to evaluate a best estimate q-factor proposed by each system's developers, without iterating to optimality.

2 INERD pin links

2.1 Modelling

A nonlinear model is developed in OpenSees (Fig. 2.1) to facilitate Incremental Dynamic Analysis for the case studies considered. The model consists of lumped plasticity elements for the members that are expected to undergo excessive deformations in the nonlinear range of the system; that primarily includes the INERD-pin links, the braces, the beams and the columns. Plastic hinges are considered at the ends of the INERD-pin links, with their properties being determined via calibration on experimental results and analytic investigations. Braces are assigned axial hinge properties in the middle of each element, while the non-dissipative elements are given hinge properties calculated according to the provisions of relevant codes (e.g. FEMA-356 [2]).

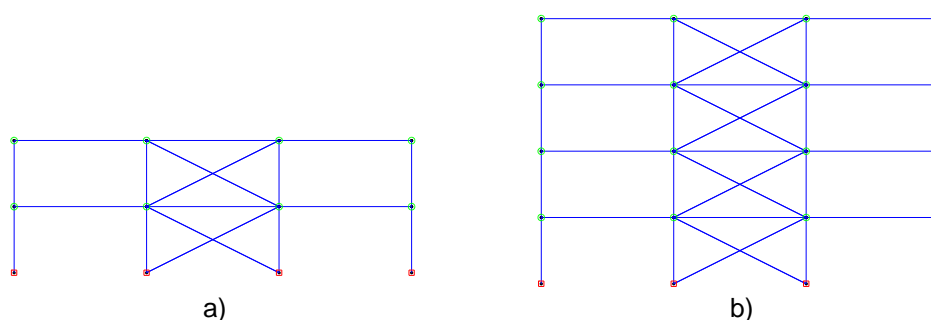


Fig. 2.1: OpenSees numerical models: a) 2-story and b) 4-story

2.2 Static Pushover Analysis

Nonlinear static analysis is performed using the aforementioned OpenSees models (Fig. 2.2). Fig. 2.3 shows their respective (1st-mode load pattern) pushover curves, where P-delta effects are taken into account. Two capacity points representing the life safety (LS) and global collapse (GC) limit states are also provided in Table 2.1. The LS capacity points have been estimated by capturing failure on an element basis.

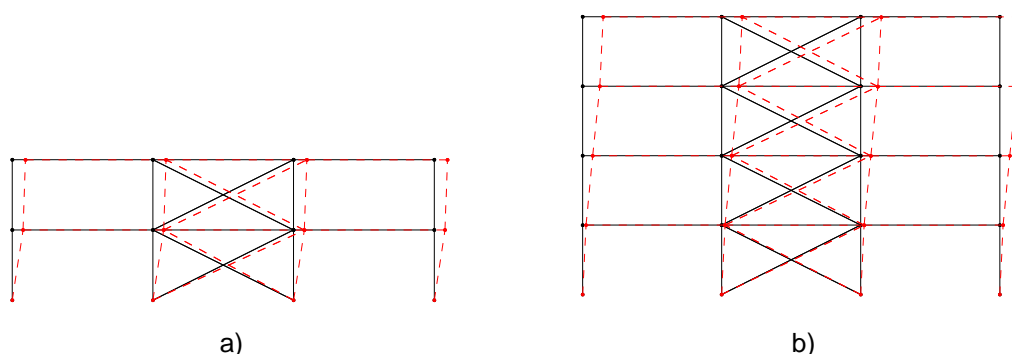


Fig. 2.2: Deflected shape: a) 2-story and b) 4-story

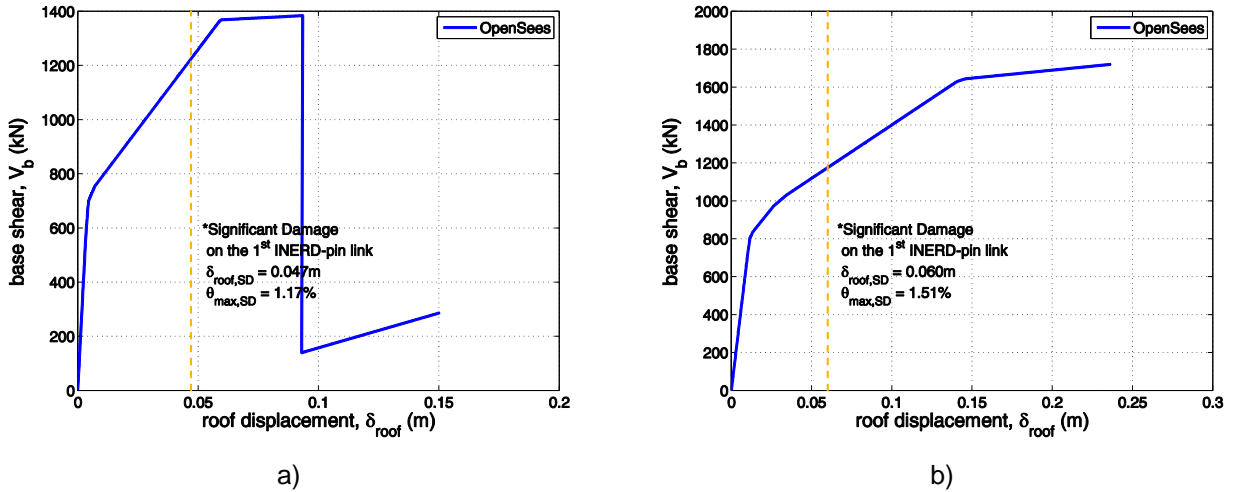


Fig. 2.3: OpenSees pushover curves: a) 2-story and b) 4-story structure

Table 2.1: Proposed acceptance criteria

Criteria	2-story		4-story	
	LS	GC	LS	GC
δ_{roof} (m)	0.047	∞	0.060	∞
θ_{max} (%)	1.17	∞	1.51	∞

2.3 Incremental Dynamic Analysis

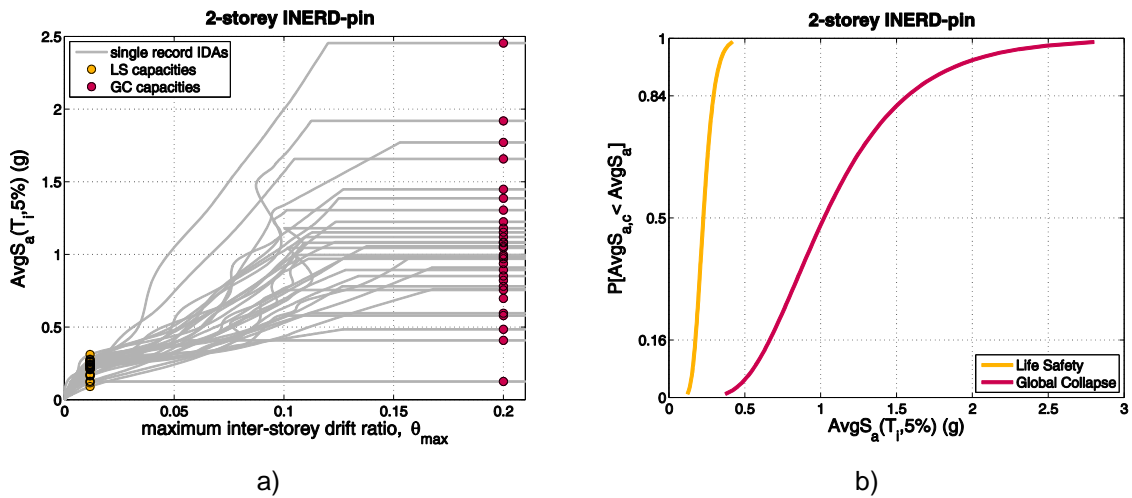


Fig. 2.4: 2-story structure: a) IDA and b) fragility curves

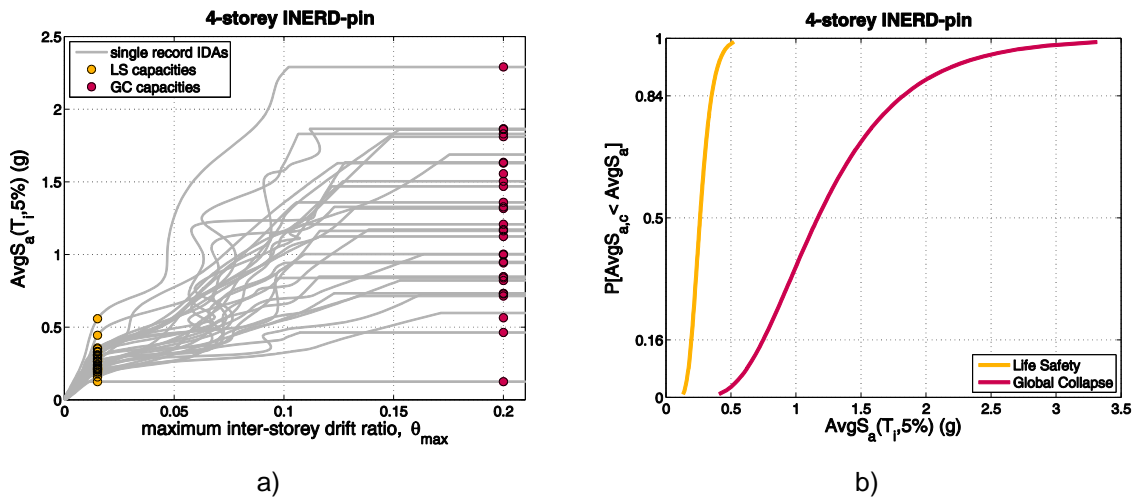


Fig. 2.5: 4-story structure: a) IDA and b) fragility curves

2.4 q-factor verification

Table 2.2: Behaviour factor verification via the limit state mean annual frequency estimation

Site	Case study	Design q-factor	Limit State	$\lambda_x(DS)$ (‰)	λ_{DSlim} (‰)	Margin Ratio ($\lambda_{lim} / \lambda_x$)	Check	Next iteration q-factor
Athens	2-story	4.0	LS	5.931	2.107	0.355	✗	2.4
			GC	0.270	0.201	0.745		
	4-story	4.0	LS	4.886	2.107	0.431	✗	
			GC	0.187	0.201	1.075		
Perugia	2-story	4.0	LS	4.862	2.107	0.433	✗	2.6
			GC	0.163	0.201	1.237		
	4-story	4.0	LS	4.787	2.107	0.440	✗	
			GC	0.131	0.201	1.531		
Perugia	2-story	4.0	LS	13.134	2.107	0.160	✗	2.0
			GC	0.095	0.201	2.122		
	4-story	4.0	LS	7.070	2.107	0.298	✗	
			GC	0.038	0.201	5.240		

3 INERD U links

3.1 Modelling

A nonlinear model is developed in the FinelG software platform (Fig. 3.1) for each of the cases studies considered. The model consists of lumped plasticity elements for the members that are expected to undergo excessive deformations in the nonlinear range of the system; that primarily includes the INERD-U links, the braces, the beams and the columns. Plastic hinges are considered at the ends of the INERD-pin links, with their properties being determined from calibration of experimental results and analytic investigations. Braces are assigned axial hinge properties in the middle of each element, while the non-dissipative elements are given hinge properties calculated according to the provisions of relevant codes (e.g. FEMA-356 [2]).

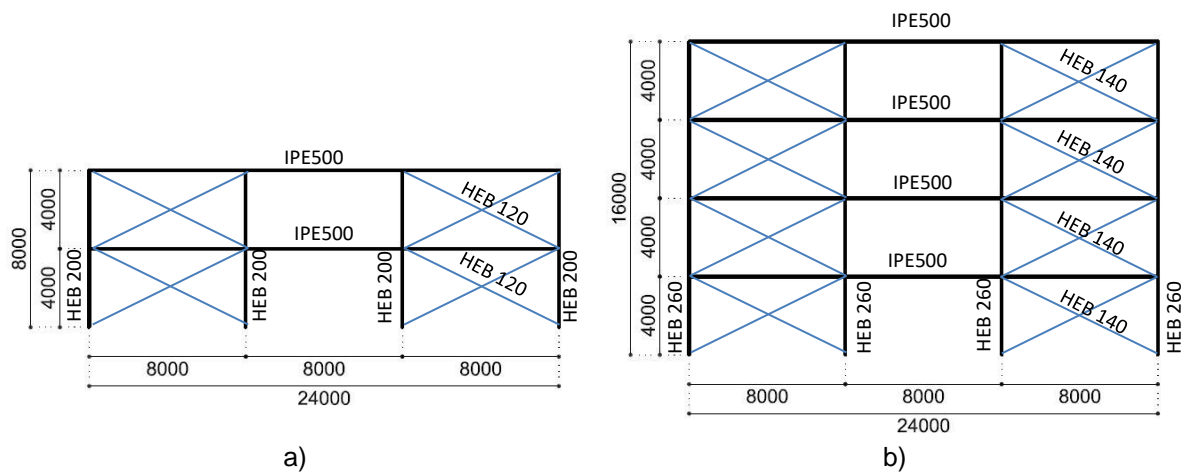


Fig. 3.1: Case studies: a) 2-story and b) 4-story

3.2 Static Pushover Analysis

Nonlinear static analysis is performed using the aforementioned models. Good matching is observed between the linear design-level model and the nonlinear model used for the pushover. The 2-story structure is clearly more ductile, while the 4-story one is more influenced by P-Delta effects, as a sharp drop appears at a ductility of about 3.

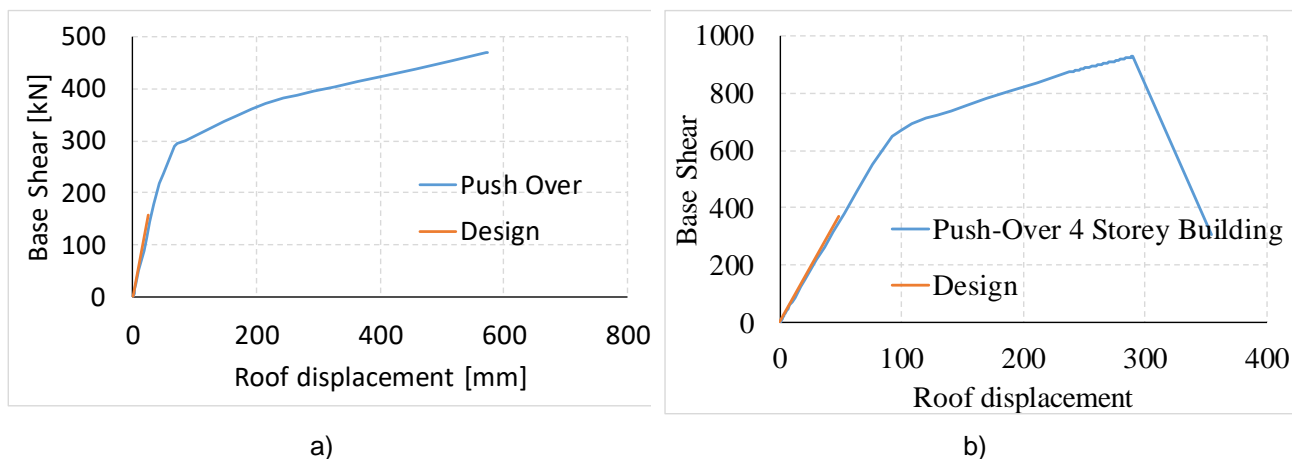


Fig. 3.2: Pushover curves: a) 2-story and b) 4-story structure

4 FUSEIS beam links

4.1 Modelling

A nonlinear model is developed in OpenSees (Fig. 4.1) to facilitate Incremental Dynamic Analysis for the case studies considered. The model consists of lumped plasticity elements for the members that are expected to undergo excessive deformations in the nonlinear range of the system; that primarily includes the FUSEIS-beam links, the beams and the columns. Plastic hinges are considered at the ends of the FUSEIS-beam links, with their properties being determined from calibration on experimental results and analytic investigations. Non-dissipative elements are given hinge properties calculated according to the provisions of relevant codes (e.g. FEMA-356 [2]).

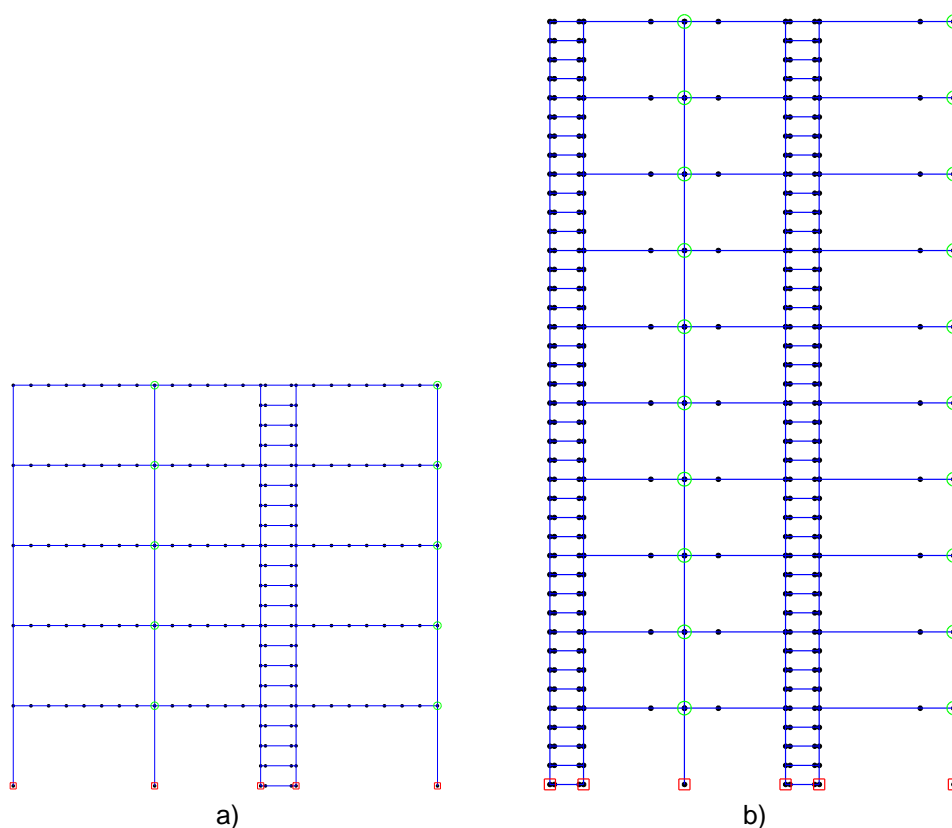


Fig. 4.1: OpenSees numerical models: a) 5-story and b) 10-story

4.2 Static Pushover Analysis

Nonlinear static analysis is performed using the aforementioned OpenSees models (Fig. 4.2). Fig. 4.3 shows their respective (1st-mode load pattern) pushover curves, where P-delta effects are taken into account. Two capacity points representing the significant damage (LS) and global collapse (GC) limit states are also provided in Table 4.1. The capacity points have been estimated by capturing failure on an element basis.

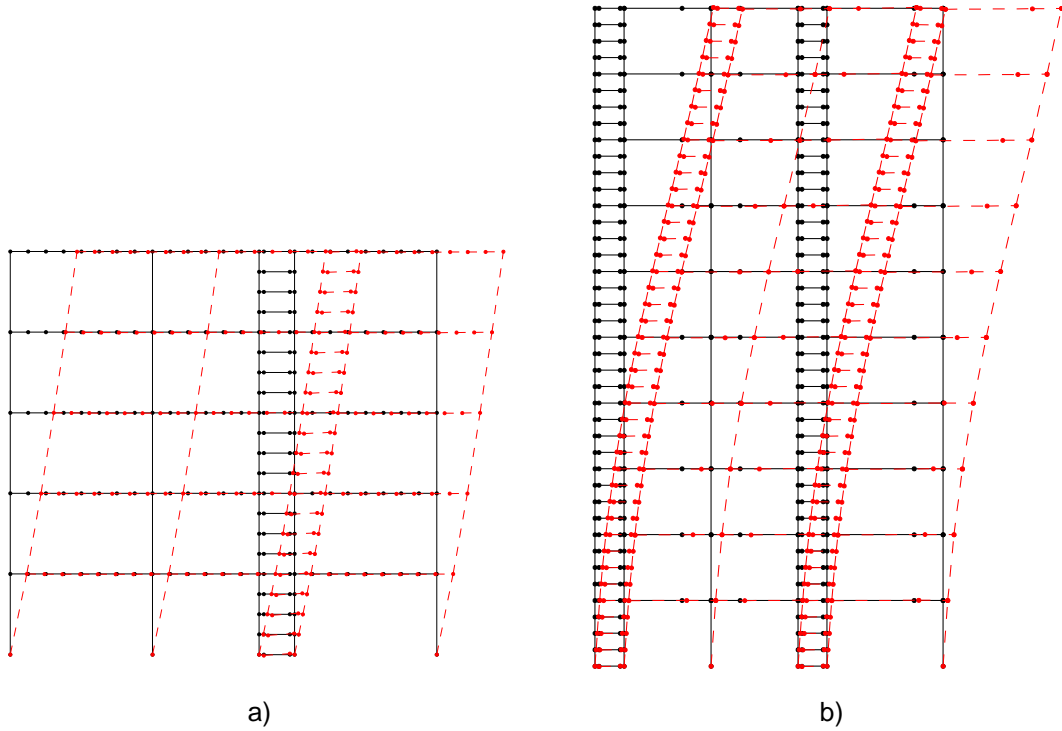
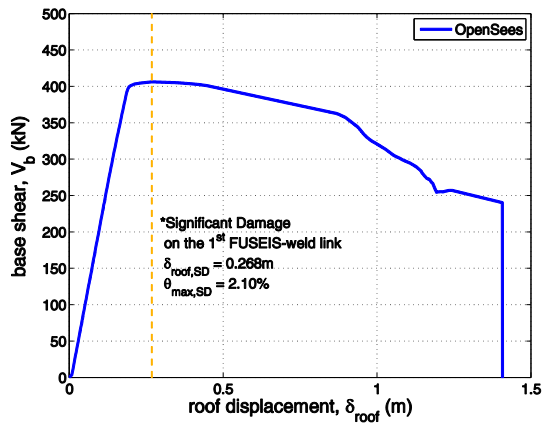
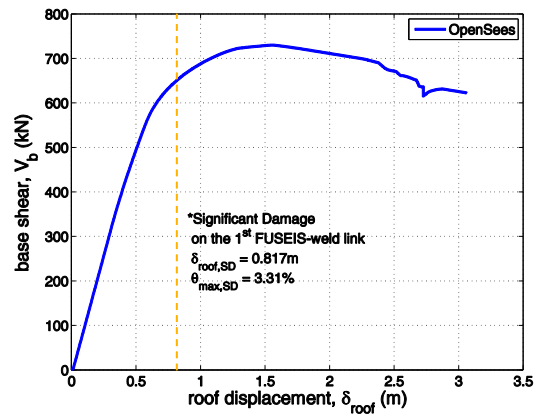


Fig. 4.2: Deflected shape: a) 5-story and b) 10-story



a)



b)

Fig. 4.3: OpenSees pushover curves: a) 5-story and b) 10-story structure

Table 4.1: Proposed acceptance criteria

Criteria	5-story		10-story	
	LS	GC	LS	GC
δ_{roof} (m)	0.268	∞	0.817	∞
θ_{max} (%)	2.09	∞	3.31	∞

4.3 Incremental Dynamic Analysis

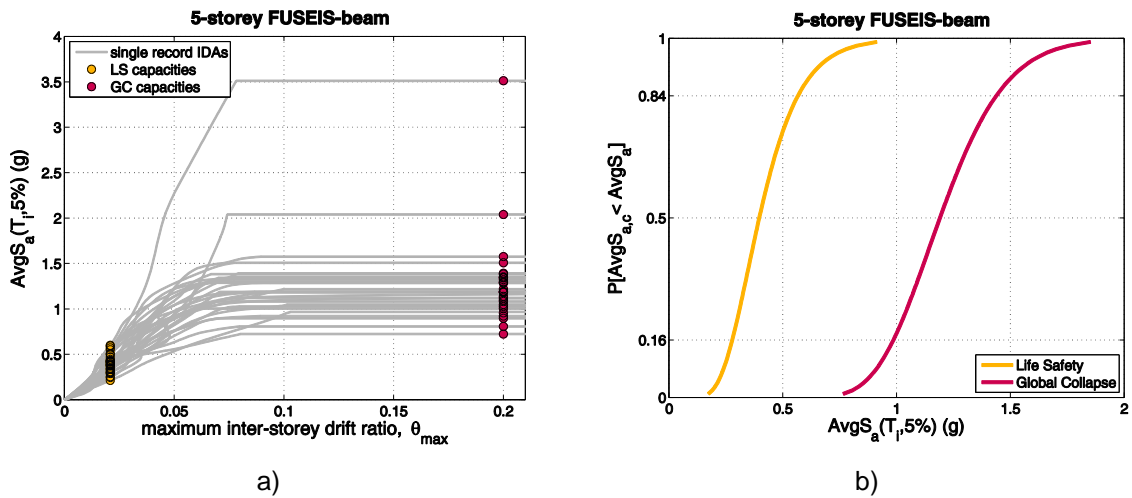


Fig. 4.4: 5-story structure: a) IDA and b) fragility curves

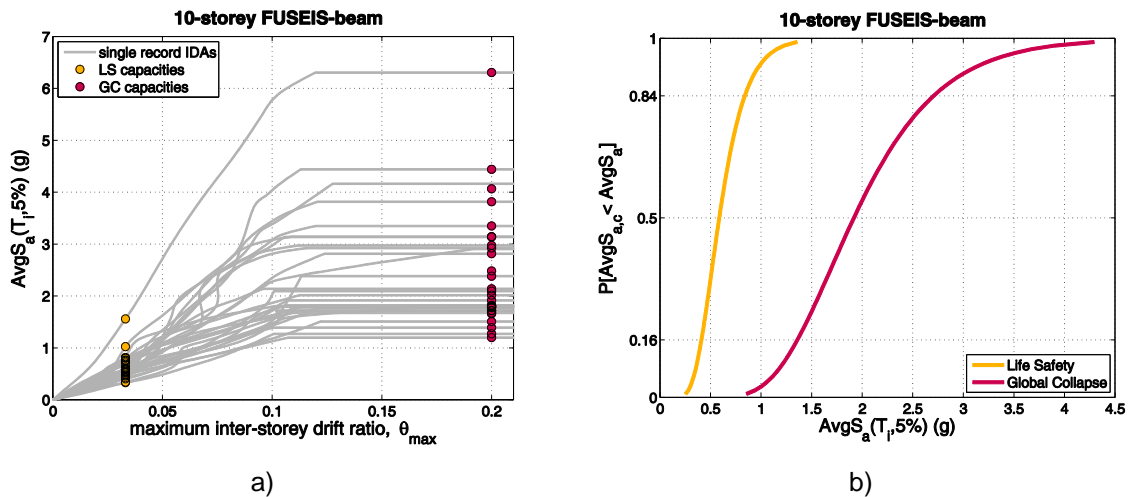


Fig. 4.5: 10-story structure: a) IDA and b) fragility curves

4.4 q-factor verification

Table 4.2: Behaviour factor verification via the limit state mean annual frequency estimation

Site	Case study	Design q-factor	Limit State	$\lambda_x(DS)$ (‰)	λ_{DSlim} (‰)	Margin Ratio ($\lambda_{lim} / \lambda_x$)	Check	Next iteration q-factor
Athens	5-story	3.5	LS	1.896	2.107	1.111	✓	-
			GC	0.061	0.201	3.308		
	10-story	5	LS	0.446	2.107	4.727	✓	-
			GC	0.008	0.201	24.148		
Perugia	5-story	3.5	LS	1.953	2.107	1.079	✓	-
			GC	0.035	0.201	5.693		
	10-story	5	LS	0.471	2.107	4.478	✓	-
			GC	0.005	0.201	39.036		
Focsani	5-story	3.5	LS	2.012	2.107	1.047	✓	-
			GC	0.000	0.201	1040.441		
	10-story	5	LS	0.171	2.107	12.338	✓	-
			GC	0.000	0.201	3518.849		

5 FUSEIS pin links

5.1 Modelling

A nonlinear model is developed in OpenSees to facilitate Incremental Dynamic Analysis for the case studies considered (Fig. 5.1). The model consists of lumped plasticity elements for the members that are expected to undergo excessive deformations in the nonlinear range of the system; that primarily includes the FUSEIS pin links, the beams as well as the columns. The beam elements representing the FUSEIS pin links are divided in three parts with different cross sections: the receptacle beams at the ends and the weakened pin in the middle. To enable the Vierendeel action, the joints between receptacle beams and system columns are simulated as rigid. Rigid zones are provided from column centres to column faces to consider their clear length in the analysis and thus exclude non-existent beam flexibilities. In this manner, the true system flexibility and strength are accounted for. Moment-rotation plastic hinges are considered at the ends of the FUSEIS pins, the properties of which are determined following the calibration of experimental results. On the other hand, the hinge properties for the non-dissipative elements are calculated according to the provisions of relevant codes (e.g. FEMA-356 [2]). In columns the interaction between bending moments and axial forces is accounted for.

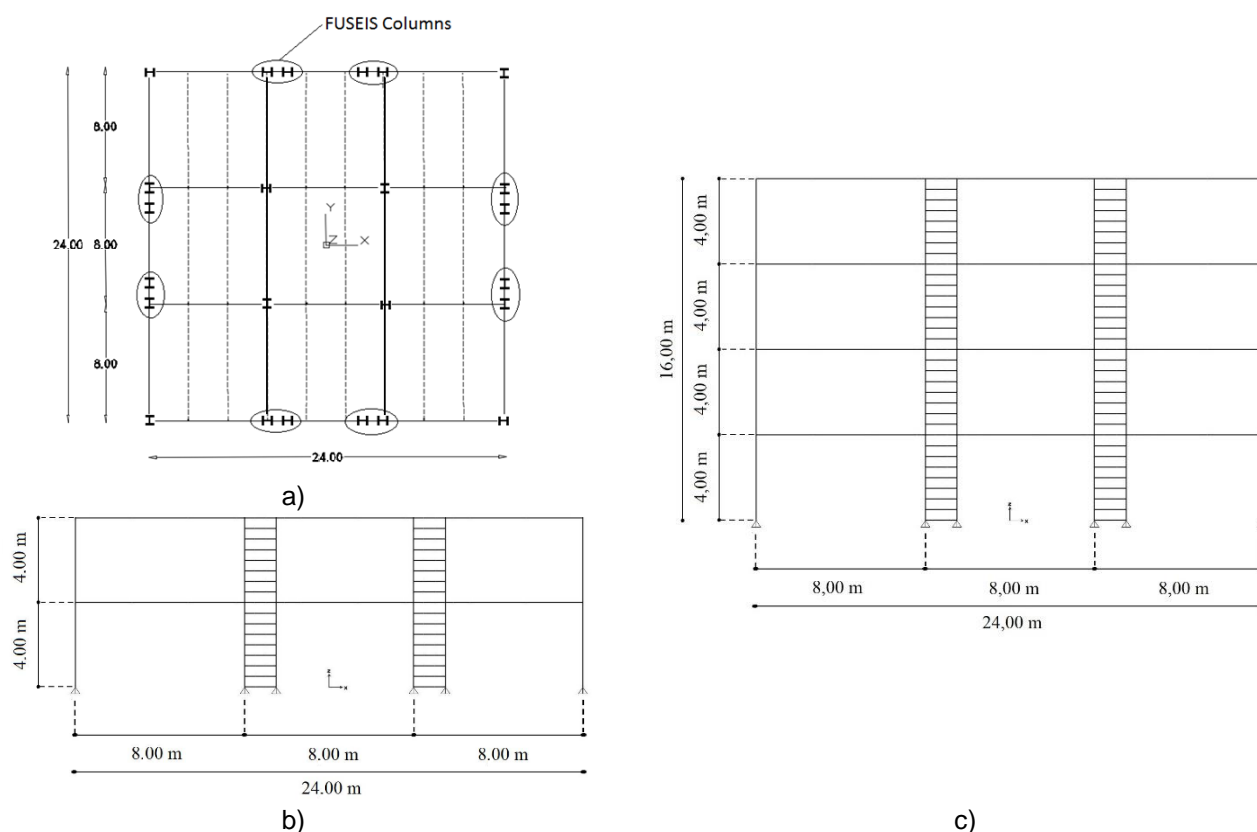


Fig. 5.1: Case-study building frames: a) Plan view, b) 2-story and c) 4-story

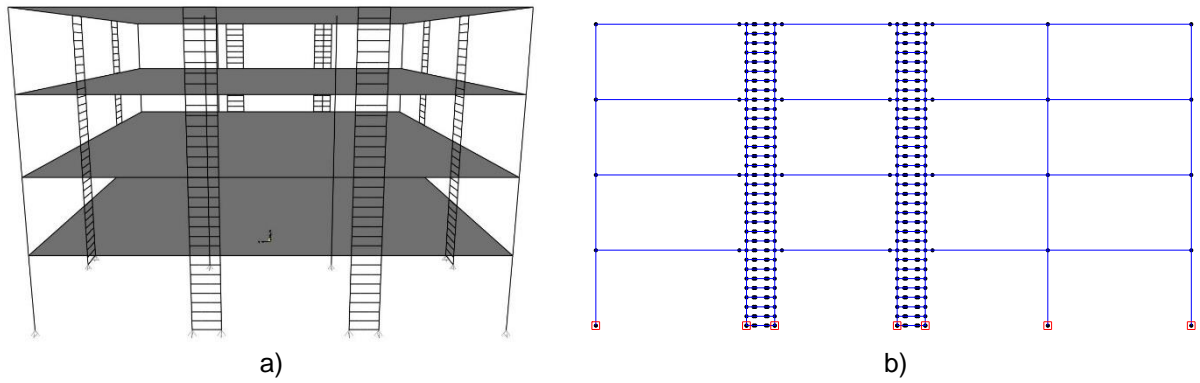


Fig. 5.2: 4-story numerical models: a) SAP2000 and b) OpenSees

5.2 Static Pushover Analysis

The OpenSees models are compared against existing SAP2000 models that were used for the design of these structures (Fig. 5.2). Fig. 5.3 and Fig. 5.4 present a comparison between the deformed shapes of the two models, while Fig. 5.5 their respective (1st-mode load pattern) pushover curves, where P-delta effects are taken into account. Two capacity points representing the significant damage (LS) and global collapse (GC) limit states are also provided in Table 5.1. The aforementioned capacity points have been estimated by capturing failure on an element basis.

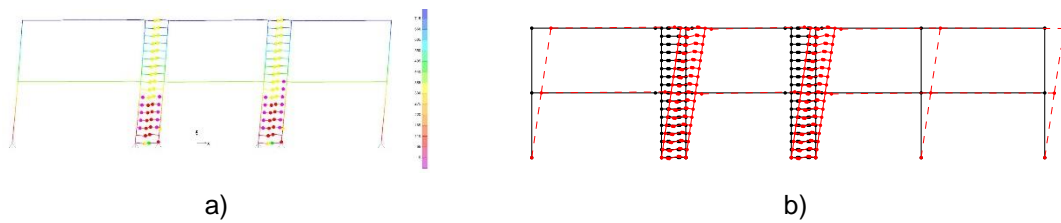


Fig. 5.3: 2-story model deflected shape: a) SAP2000 and b) OpenSees

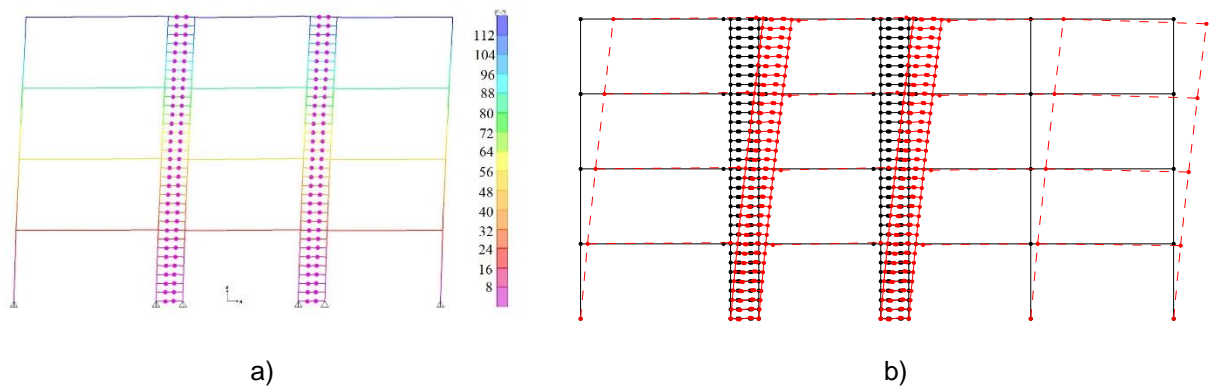


Fig. 5.4: 4-story model deflected shape: a) SAP2000 and b) OpenSees

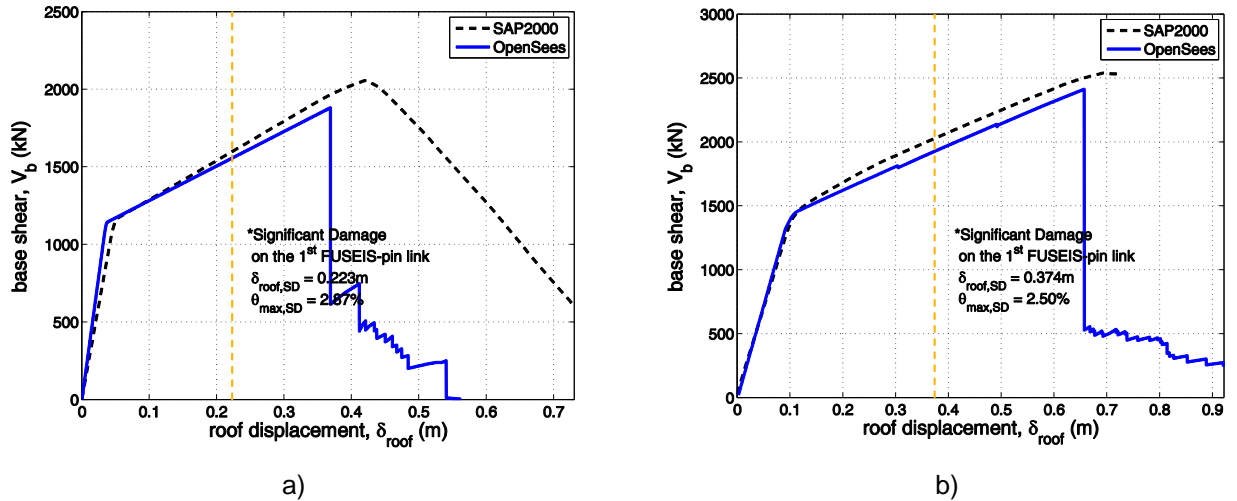


Fig. 5.5: OpenSees versus SAP2000 pushover curves: a) 2-story and b) 4-story structure

Table 5.1: Proposed acceptance criteria

Criteria	2-story		4-story	
	LS	GC	LS	GC
δ_{roof} (m)	0.223	∞	0.374	∞
θ_{max} (%)	2.87	∞	2.50	∞

5.3 Incremental Dynamic Analysis

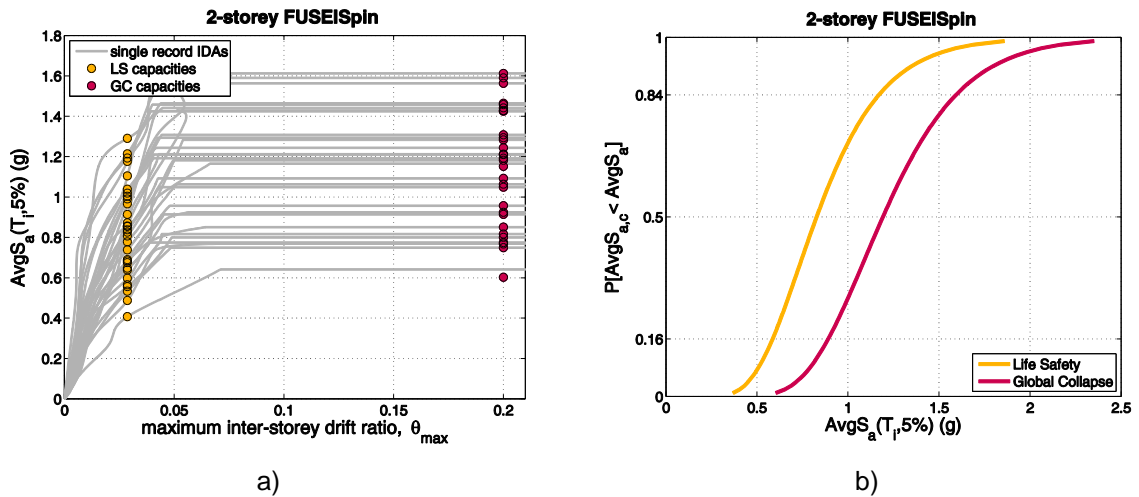


Fig. 5.6: 2-story structure: a) IDA and b) fragility curves

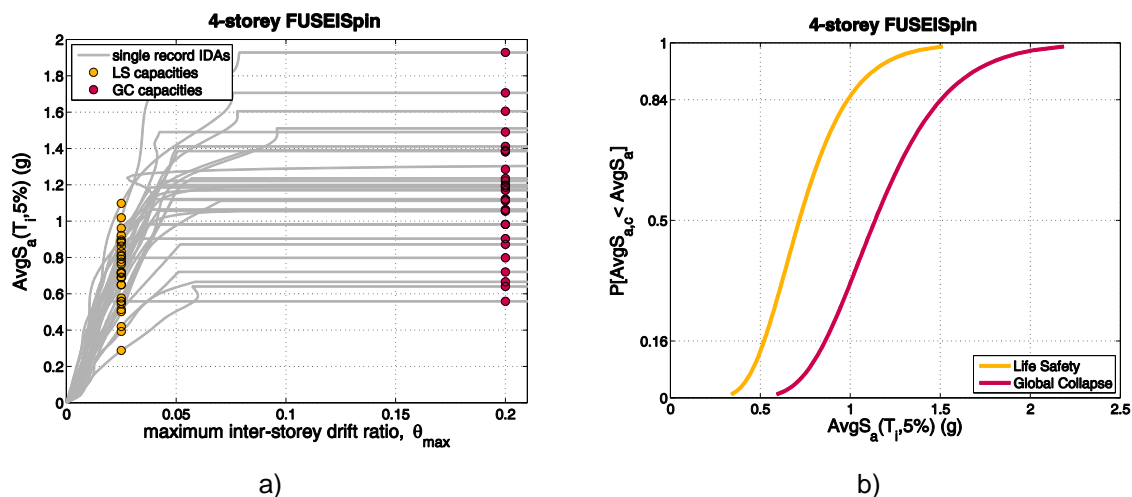


Fig. 5.7: 4-story structure: a) IDA and b) fragility curves

5.4 q-factor verification

Table 5.2: Behaviour factor verification via the limit state mean annual frequency estimation

Site	Case study	Design q-factor	Limit State	$\lambda_x(DS)$ (‰)	λ_{Dslim} (‰)	Margin Ratio ($\lambda_{lim} / \lambda_x$)	Check	Next iteration q-factor
Athens	2-story	3	LS	0.295	2.107	7.144	✓	-
			GC	0.100	0.201	2.014		
	4-story	3	LS	0.409	2.107	5.158	✓	-
			GC	0.106	0.201	1.903		
Perugia	2-story	3	LS	0.175	2.107	12.074	✓	-
			GC	0.049	0.201	4.080		
	4-story	3	LS	0.296	2.107	7.110	✓	-
			GC	0.062	0.201	3.248		
Focsani	2-story	3	LS	0.061	2.107	34.469	✓	-
			GC	0.004	0.201	48.046		
	4-story	3	LS	0.078	2.107	26.917	✓	-
			GC	0.003	0.201	61.759		

6 FUSEIS bolted cover plate links

6.1 Modelling

A nonlinear model is developed in OpenSees to facilitate Incremental Dynamic Analysis for the case studies considered (Fig. 6.2). The model consists of lumped plasticity elements for the members that are expected to undergo excessive deformations in the nonlinear range of the system; that primarily includes the FUSEIS bolted links, the beams as well as the columns. Moment-rotation plastic hinges are considered at the ends of the FUSEIS bolted links, with their properties being determined from calibration of experimental results and analytic investigations. On the other hand, the hinge properties for the non-dissipative elements are calculated according to the provisions of relevant codes (e.g. FEMA-356 [2]). In columns the interaction between bending moments and axial forces is accounted for.

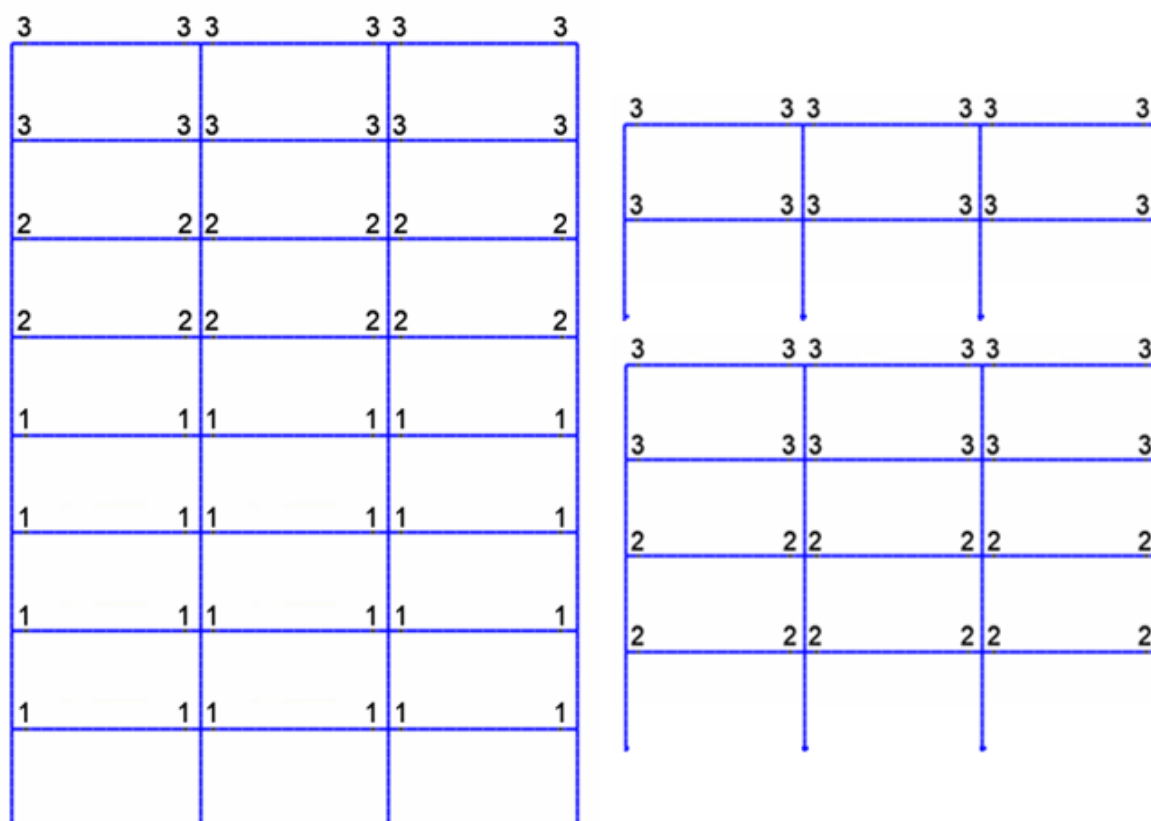


Fig. 6.1: Distribution of assigned bolted beam splices

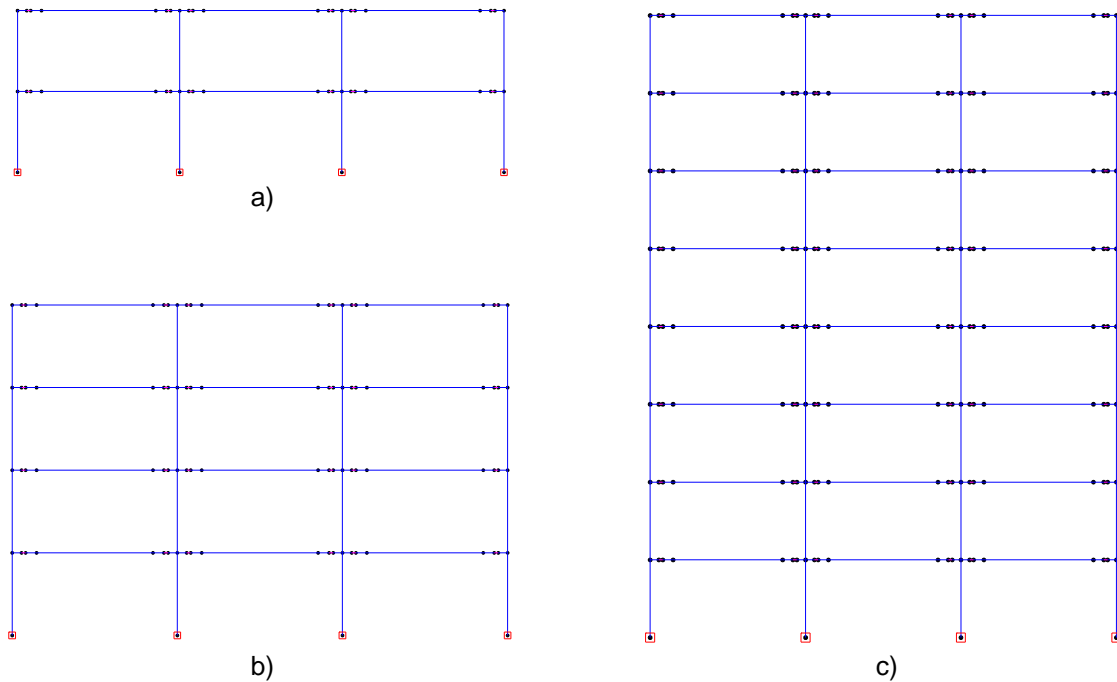


Fig. 6.2: OpenSees numerical models: a) 2-story, b) 4-story and c) 8-story

6.2 Static Pushover Analysis

The OpenSees models are compared against existing SAP2000 models that were used for the design of these structures (Fig. 6.2). Fig. 6.3, Fig. 6.4 and Fig. 6.5 present a comparison between the deformed shapes of the three models, while Fig. 6.6 their respective (1st-mode load pattern) pushover curves, where P-delta effects are taken into account. Two capacity points representing the significant damage (LS) and global collapse (GC) limit states are also provided in Table 6.1. The aforementioned capacity points have been estimated by capturing failure on an element basis.

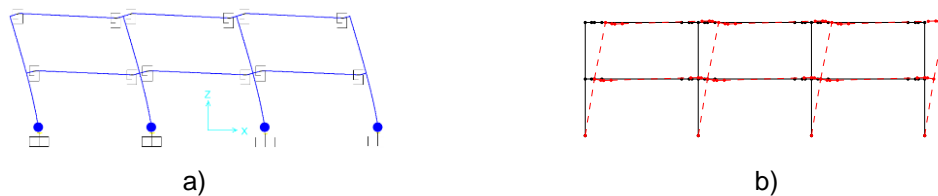


Fig. 6.3: 2-story model deflected shape: a) SAP2000 and b) OpenSees

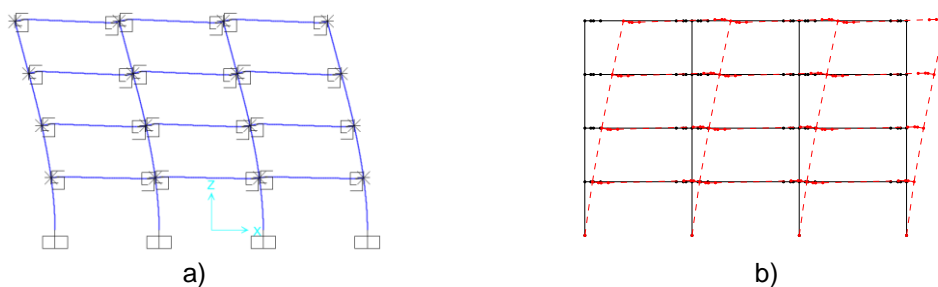


Fig. 6.4: 4-story model deflected shape: a) SAP2000 and b) OpenSees

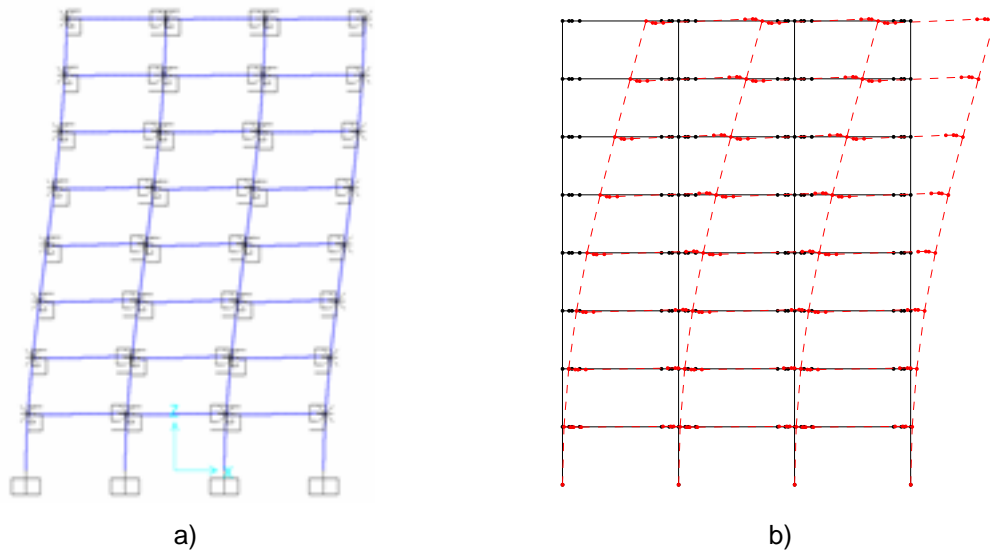


Fig. 6.5: 8-story model deflected shape: a) SAP2000 and b) OpenSees

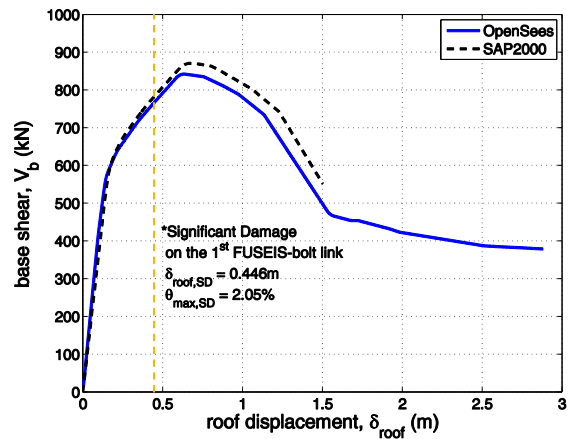
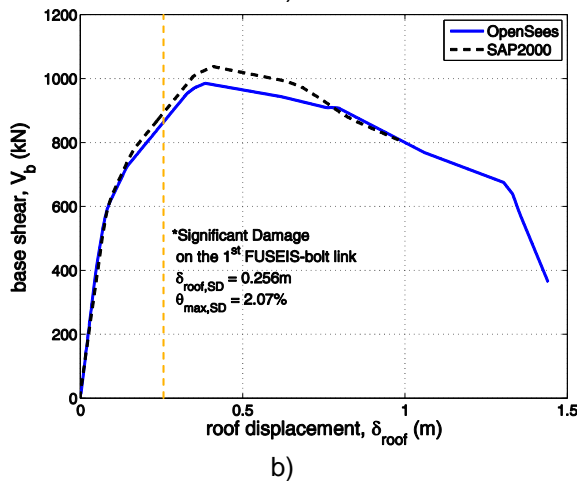
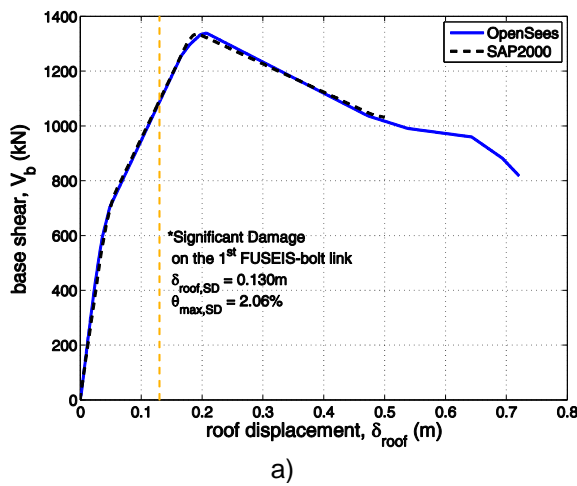


Fig. 6.6: OpenSees versus SAP2000 pushover curves: a) 2-story, b) 4-story and c) 8-story

Table 6.1: Proposed acceptance criteria

Criteria	2-story		4-story		8-story	
	LS	GC	LS	GC	LS	GC
δ_{roof} (m)	0.130	∞	0.256	∞	0.446	∞
θ_{max}	2.06	∞	2.07	∞	2.05	∞

6.3 Incremental Dynamic Analysis

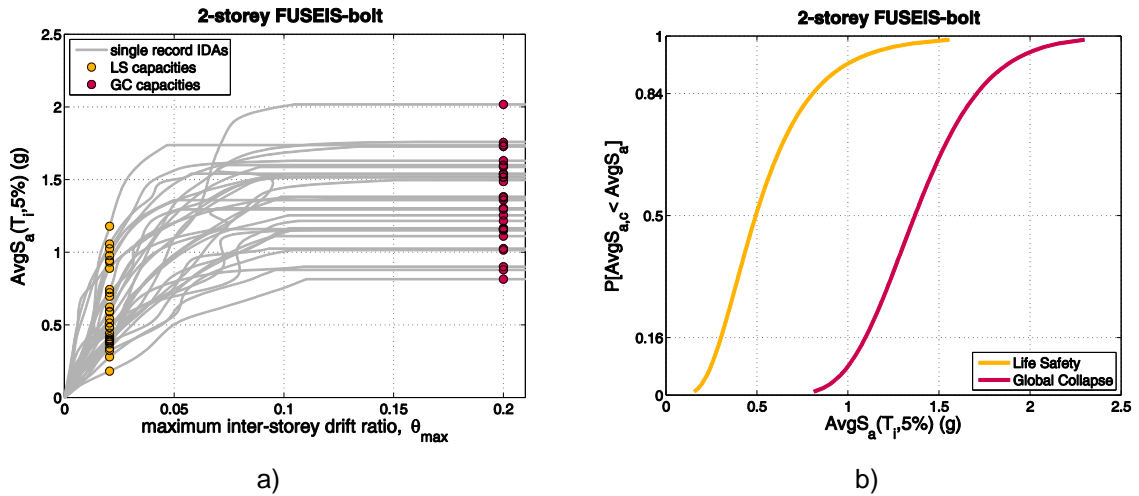


Fig. 6.7: 2-story structure: a) IDA and b) fragility curves

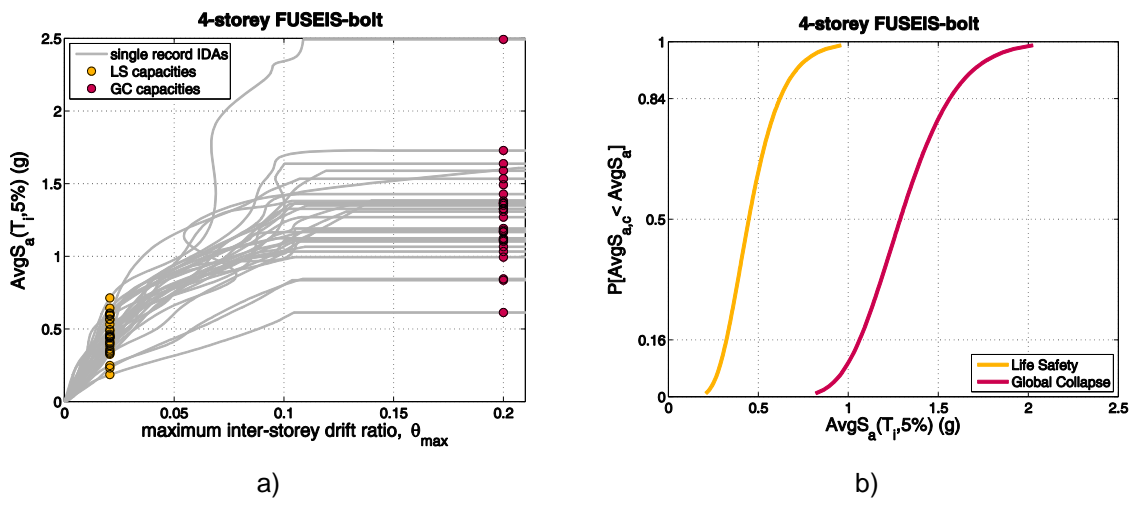


Fig. 6.8: 4-story structure: a) IDA and b) fragility curves

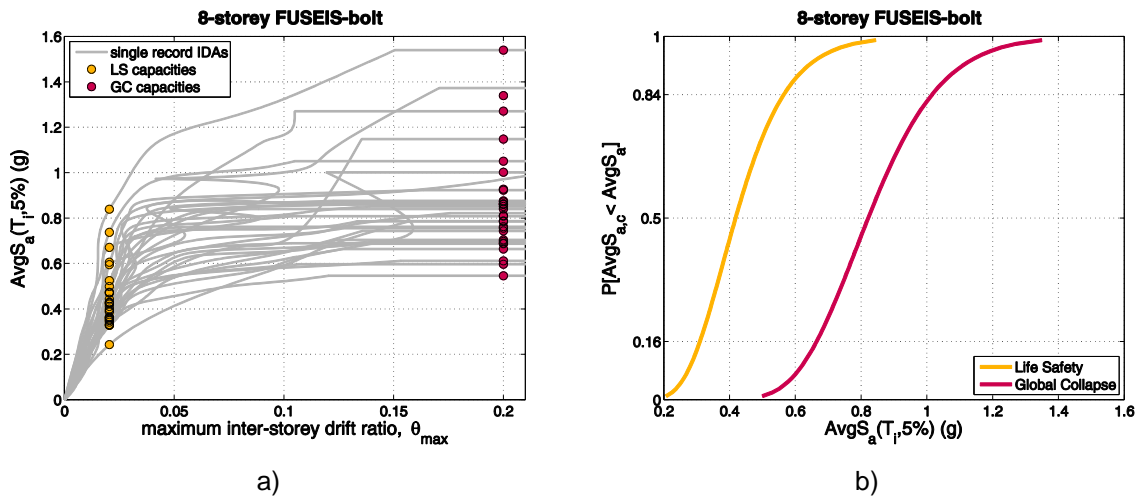


Fig. 6.9: 8-story structure: a) IDA and b) fragility curves

6.4 q-factor verification

Table 6.2: Behaviour factor verification via the limit state mean annual frequency estimation

Site	Case study	Design q-factor	Limit State	$\lambda_x(DS)$ (‰)	λ_{DSlim} (‰)	Margin Ratio ($\lambda_{lim} / \lambda_x$)	Check	Next iteration q-factor
Athens	2-story	4	LS	1.639	2.107	1.286	✓	-
			GC	0.041	0.201	4.944		
	4-story	4	LS	1.415	2.107	1.489	✓	-
			GC	0.048	0.201	4.176		
	8-story	4	LS	1.536	2.107	1.372	✗	3.6
			GC	0.247	0.201	0.813		
Perugia	2-story	4	LS	1.340	2.107	1.573	✓	-
			GC	0.018	0.201	11.307		
	4-story	4	LS	1.259	2.107	1.673	✓	-
			GC	0.024	0.201	8.245		
	8-story	4	LS	1.605	2.107	1.313	✓	-
			GC	0.192	0.201	1.047		
Focsani	2-story	4	LS	1.906	2.107	1.106	✓	-
			GC	0.000	0.201	1677.86		
	4-story	4	LS	0.932	2.107	2.262	✓	-
			GC	0.000	0.201	2134.39		
	8-story	4	LS	1.210	2.107	1.741	✓	-
			GC	0.018	0.201	10.954		

7 FUSEIS welded cover plate links

7.1 Modelling

A nonlinear model is developed in OpenSees (Fig. 7.1) to facilitate Incremental Dynamic Analysis for the case studies considered (Fig. 7.2, Fig. 7.3, Fig. 7.4). The model consists of lumped plasticity elements for the members that are expected to undergo excessive deformations in the nonlinear range of the system; that primarily includes the FUSEIS bolted links, the beams as well as the columns. Moment-rotation plastic hinges are considered at the ends of the FUSEIS bolted links, with their properties being determined from calibration of experimental results and analytic investigations. On the other hand, the hinge properties for the non-dissipative elements are calculated according to the provisions of relevant codes (e.g. FEMA-356 [2]). In columns the interaction between bending moments and axial forces is accounted for.

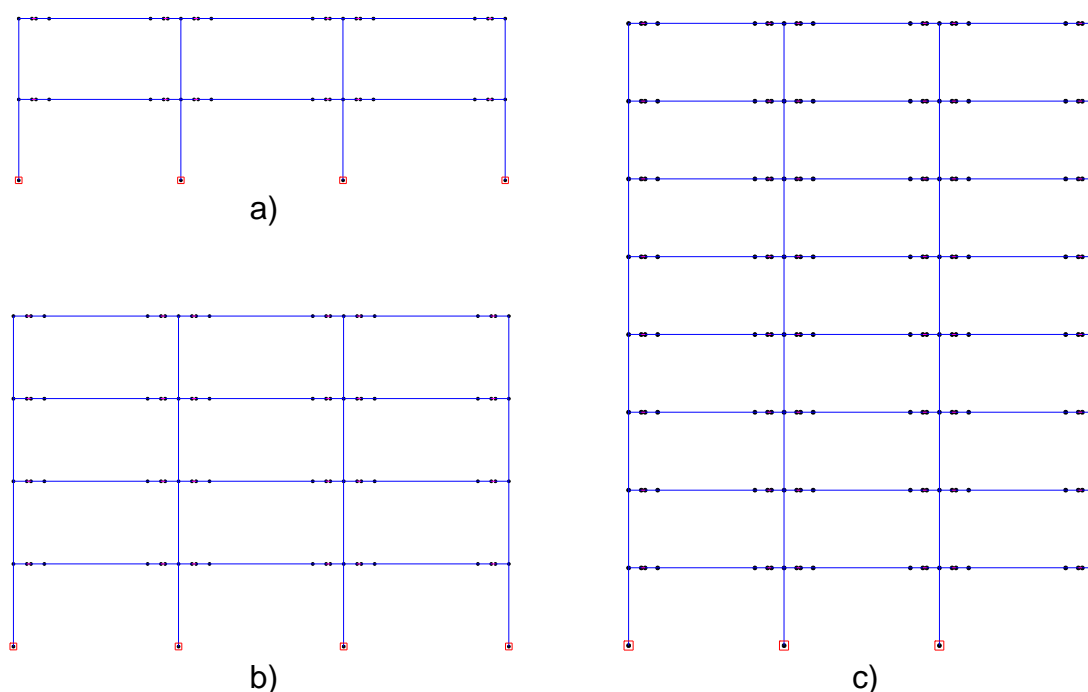


Fig. 7.1: OpenSees numerical models: a) 2-story, b) 4-story and c) 8-story

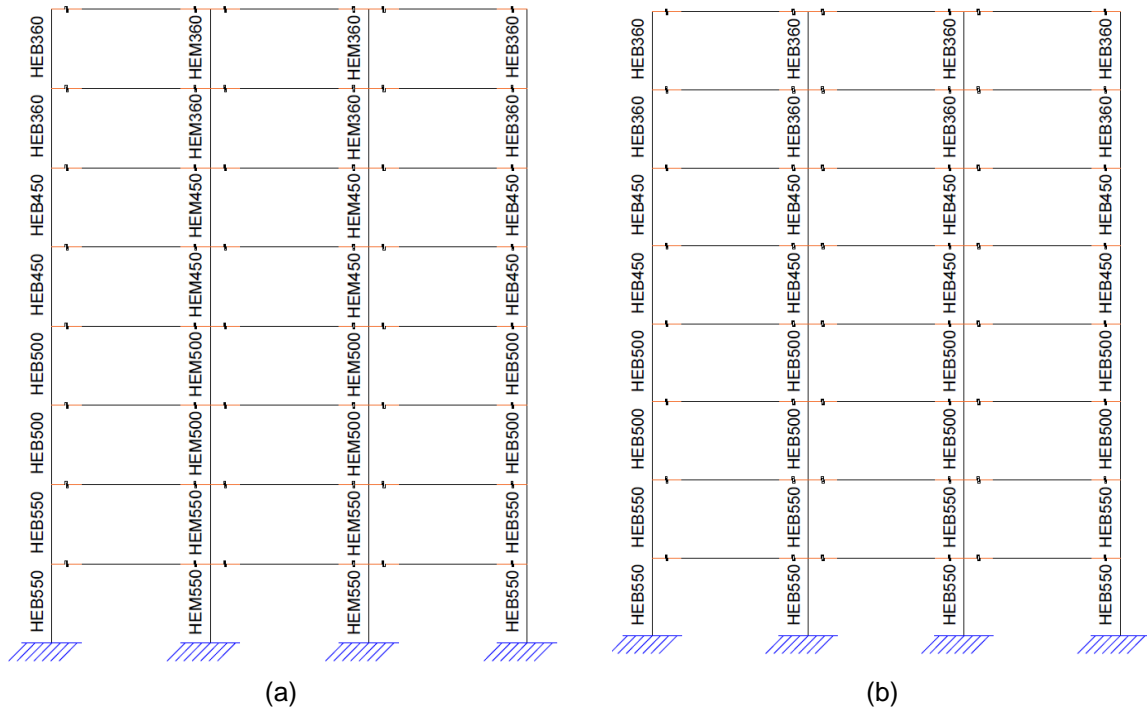


Fig. 7.2: Side view of the modelled building: (a) internal frames and (b) external frames. The reinforced beam zones are highlighted in orange in which the marks that represent the welded FUSEIS can be observed.

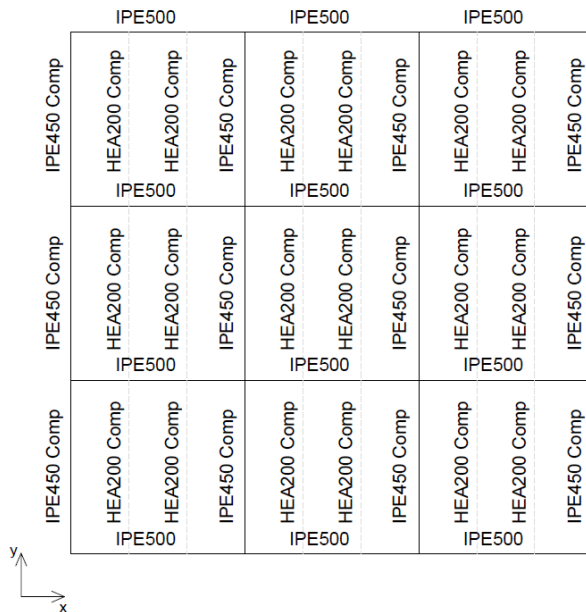


Fig. 7.3: Plan view of the modelled building (the reinforced beam zones and the welded FUSEIS are not represented)

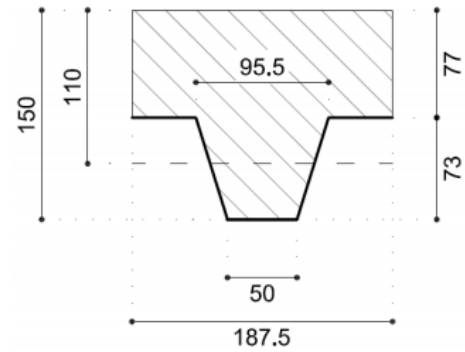


Fig. 7.4: Schematic representation of the composite slab

7.2 Static Pushover Analysis

The OpenSees models are compared against existing SAP2000 models that were used for the design of these structures (Fig. 7.1). Fig. 7.5 and Fig. 7.6 present a comparison between the deformed shapes of the three models, while Fig. 7.7 their respective (1st-mode load pattern) pushover curves, where P-delta effects are taken into account. Two capacity points representing the significant damage (LS) and global collapse (GC) limit states are also provided in Table 7.1. The aforementioned capacity points have been estimated by capturing failure on an element basis.

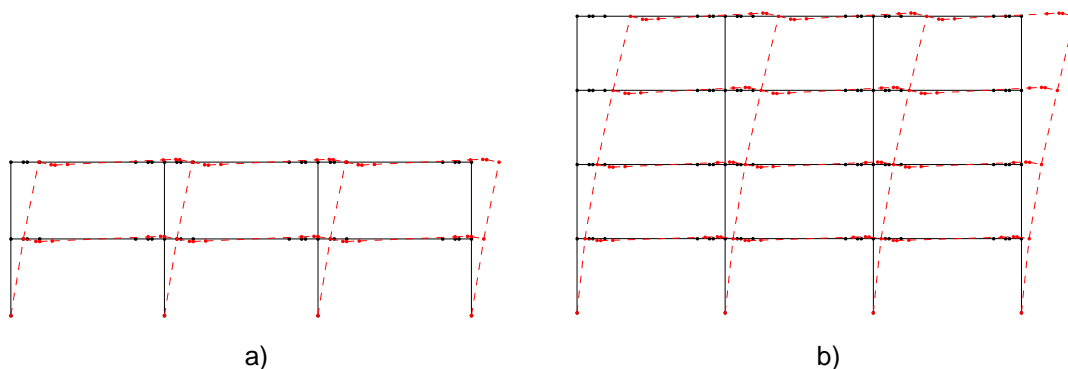


Fig. 7.5: OpenSees models: a) 2-story and b) 4-story

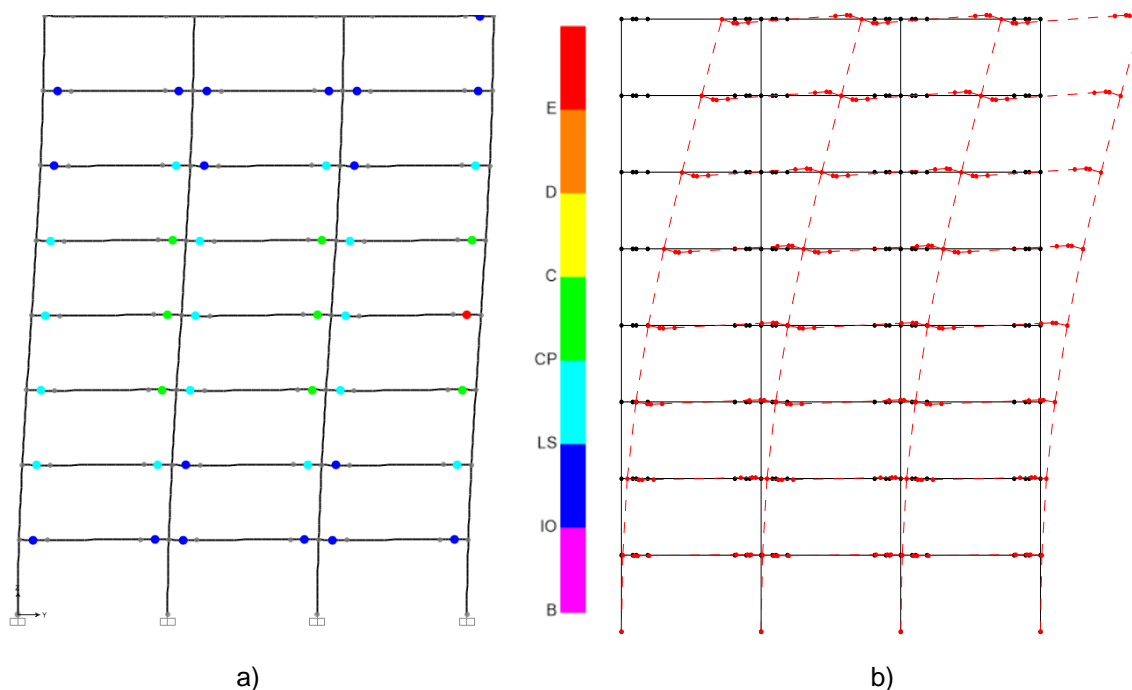


Fig. 7.6: 8-story model deflected shape: a) SAP2000 and b) OpenSees

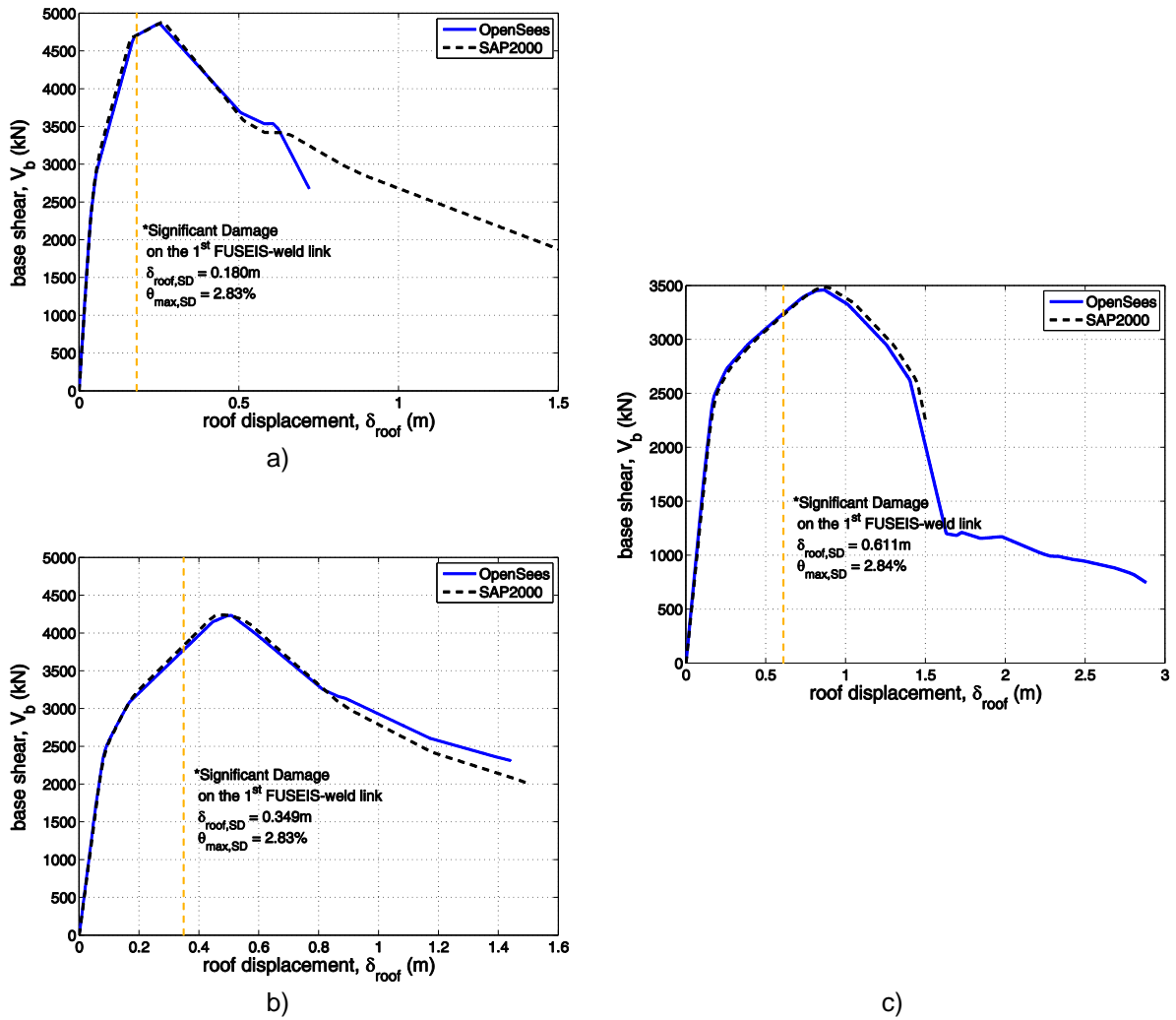


Fig. 7.7: OpenSees versus SAP2000 pushover curves: a) 2-story, b) 4-story and c) 8-story

Table 7.1: Proposed acceptance criteria

Criteria	2-story		4-story		8-story	
	LS	GC	LS	GC	LS	GC
$\bar{\delta}_{roof}$ (m)	0.180	∞	0.349	∞	0.611	∞
θ_{max} (%)	2.83	∞	2.83	∞	2.84	∞

7.3 Incremental Dynamic Analysis

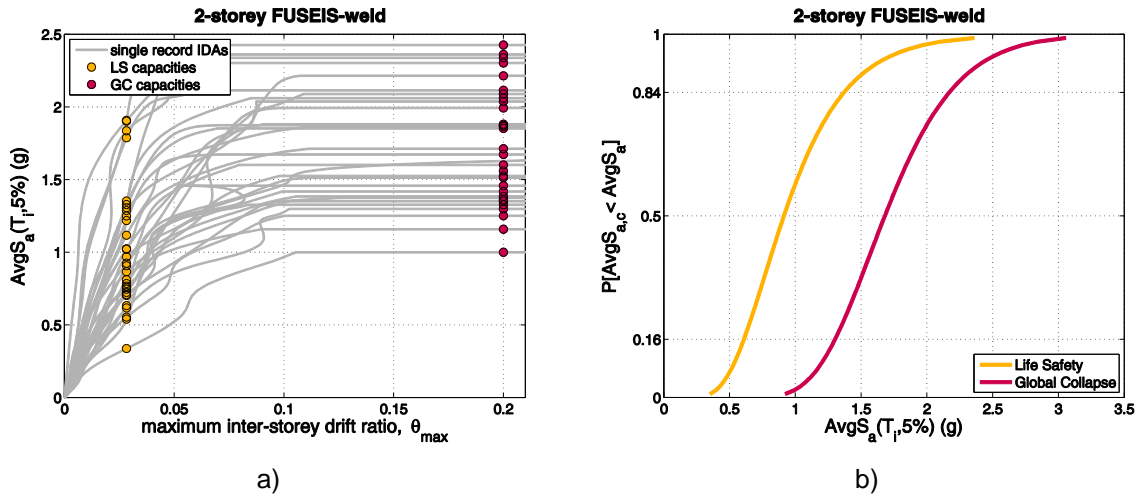


Fig. 7.8: 2-story structure: a) IDA and b) fragility curves

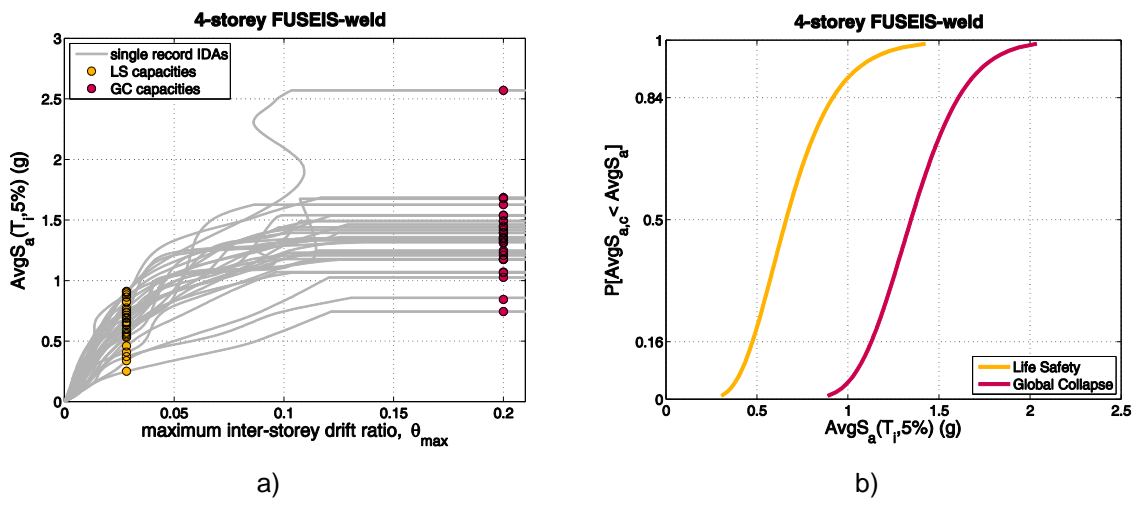


Fig. 7.9: 4-story structure: a) IDA and b) fragility curves

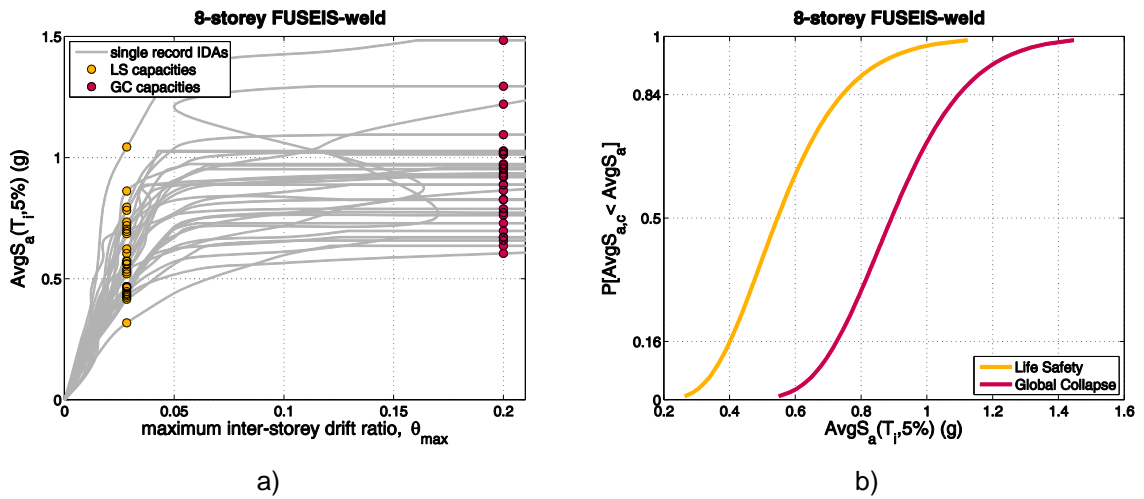


Fig. 7.10: 8-story structure: a) IDA and b) fragility curves

7.4 q-factor verification

Table 7.2: Behaviour factor verification via the limit state mean annual frequency estimation

Site	Case study	Design q-factor	Limit State	$\lambda_x(DS)$ (‰)	λ_{DSlim} (‰)	Margin Ratio ($\lambda_{lim} / \lambda_x$)	Check	Next iteration q-factor
Athens	2-story	4	LS	0.277	2.107	7.614	✓	-
			GC	0.020	0.201	10.255		
	4-story	4	LS	0.542	2.107	3.887	✓	-
			GC	0.038	0.201	5.329		
	8-story	4	LS	0.813	2.107	2.591	✓	-
			GC	0.196	0.201	1.028		
Perugia	2-story	4	LS	0.164	2.107	12.813	✓	-
			GC	0.007	0.201	27.875		
	4-story	4	LS	0.410	2.107	5.144	✓	-
			GC	0.017	0.201	11.507		
	8-story	4	LS	0.776	2.107	2.714	✓	-
			GC	0.145	0.201	1.384		
Focsani	2-story	4	LS	0.080	2.107	26.471	✓	-
			GC	0.000	0.201	4930.03		
	4-story	4	LS	0.141	2.107	14.935	✓	-
			GC	0.000	0.201	10352.61		
	8-story	4	LS	0.375	2.107	5.621	✓	-
			GC	0.010	0.201	20.831		

8 DUAREM removable link devices

8.1 Modelling

A nonlinear model is developed in OpenSees (Fig. 8.1) to facilitate Incremental Dynamic Analysis for the case studies considered (Fig. 8.2). The model consists of lumped plasticity elements for the members that are expected to undergo excessive deformations in the nonlinear range of the system; that primarily includes the DUAREM links, the braces, the beams and the columns. Shear force-displacement plastic hinges are considered at the ends of the DUAREM links, with their properties being determined from calibration of experimental results and analytic investigations. Braces are assigned axial “hinge” properties in the middle of each element, while the non-dissipative elements are given hinge properties calculated according to the provisions of relevant codes (e.g. FEMA-356 [2]).

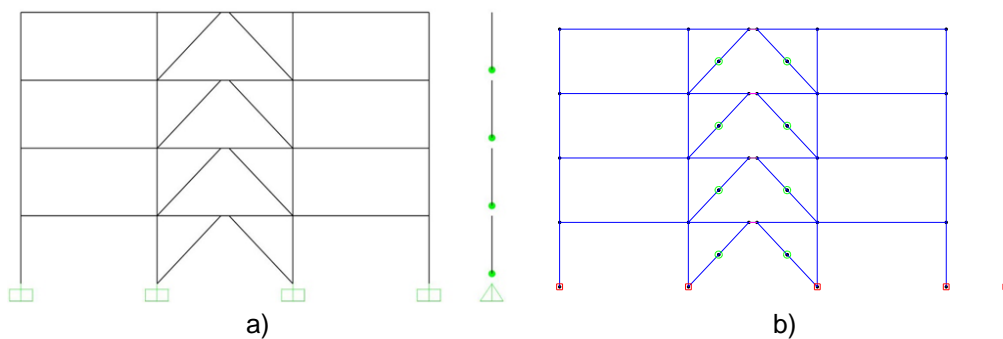


Fig. 8.1: 4-story numerical models: a) SAP2000 and b) Opensees

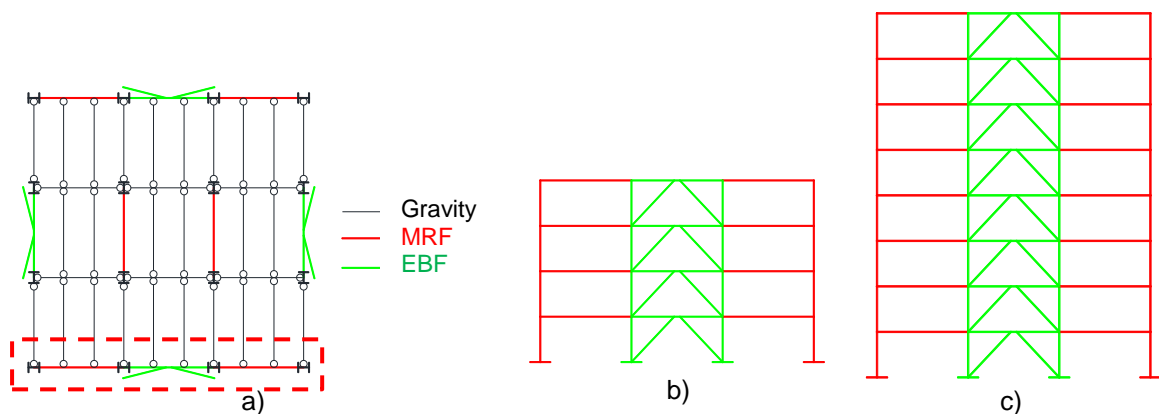
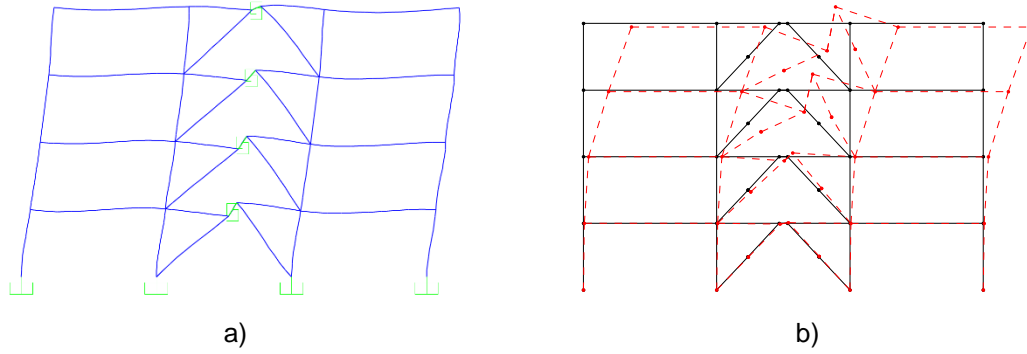


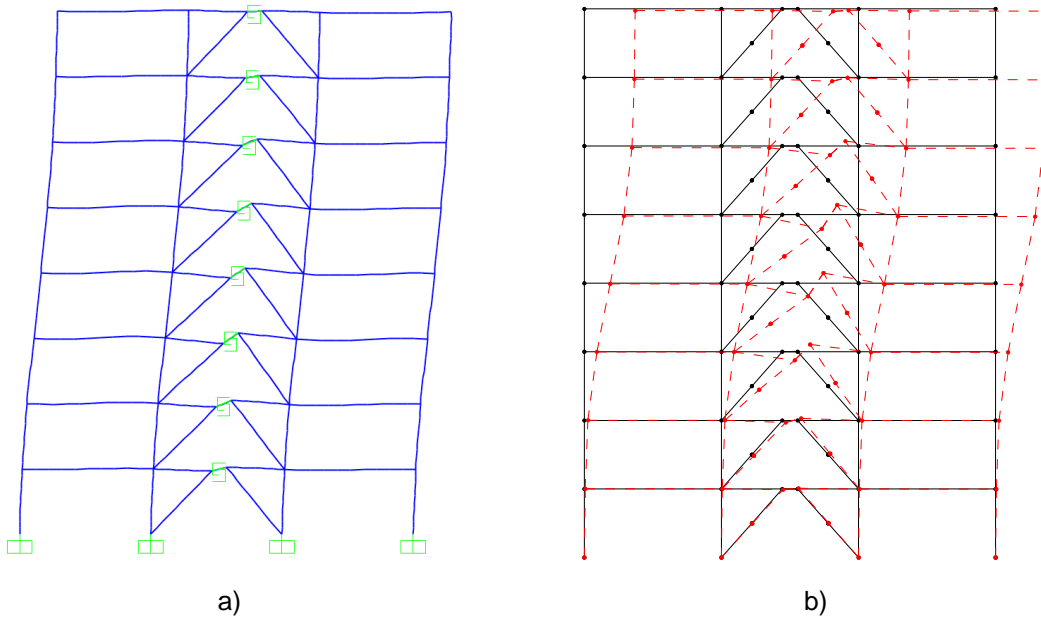
Fig. 8.2: Case-study building frames: a) Plan view, b) 4-story and c) 8-story

8.2 Static Pushover Analysis

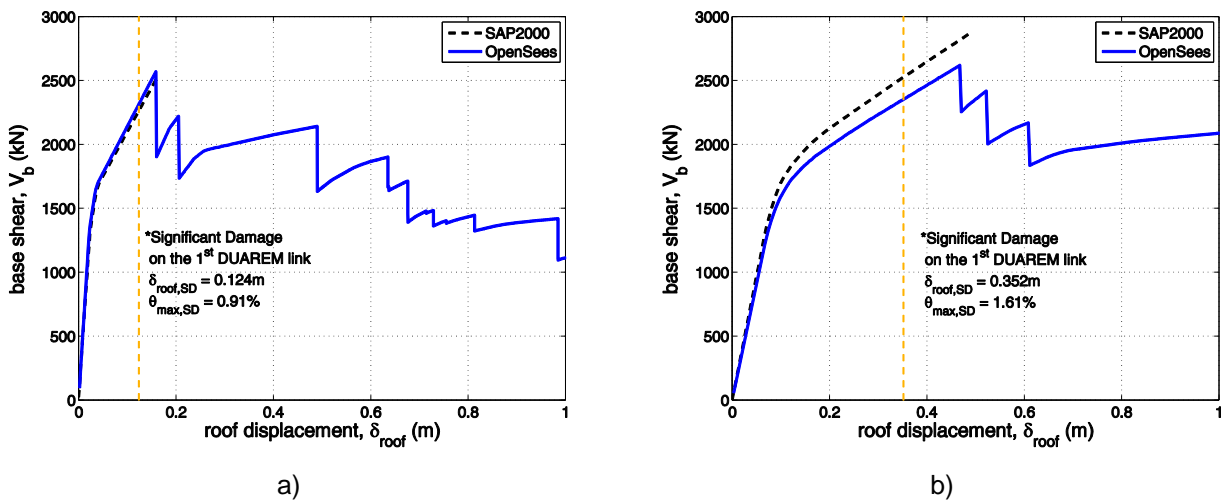
The OpenSees models are compared against existing SAP2000 models that were used for the design of these structures (Fig. 8.1a). Fig. 8.3 and Fig. 8.4 present a comparison between the deformed shapes of the three models, while Fig. 8.5 their respective (1st-mode load pattern) pushover curves, where P-delta effects are taken into account. Two capacity points representing the significant damage (LS) and global collapse (GC) limit states are also provided in Table 8.1. The aforementioned capacity points have been estimated by capturing failure on an element basis.



a) b)
Fig. 8.3: 4-story model deflected shape: a) SAP2000 and b) OpenSees



a) b)
Fig. 8.4: 8-story model deflected shape: a) SAP2000 and b) OpenSees

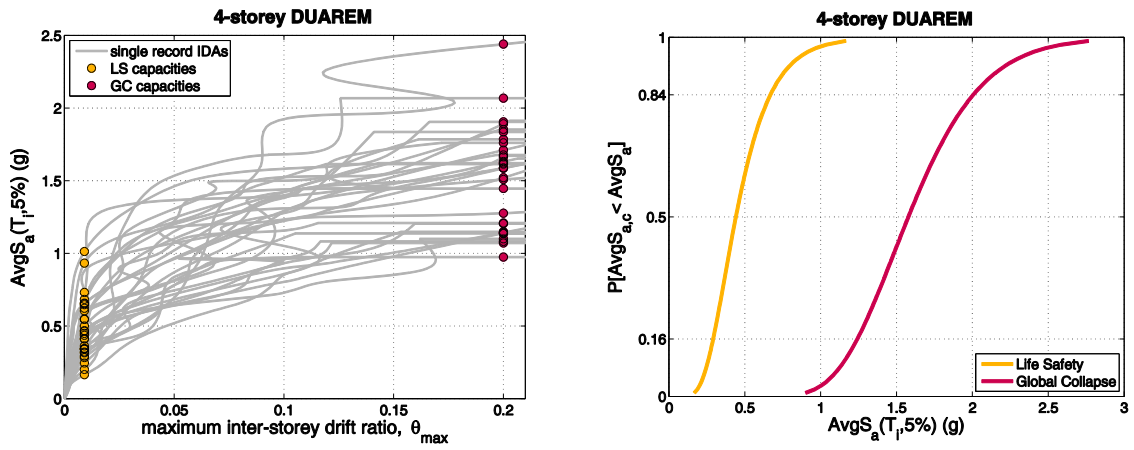


a) b)
Fig. 8.5: OpenSees versus SAP2000 pushover curves: a) 4-story and b) 8-story structure

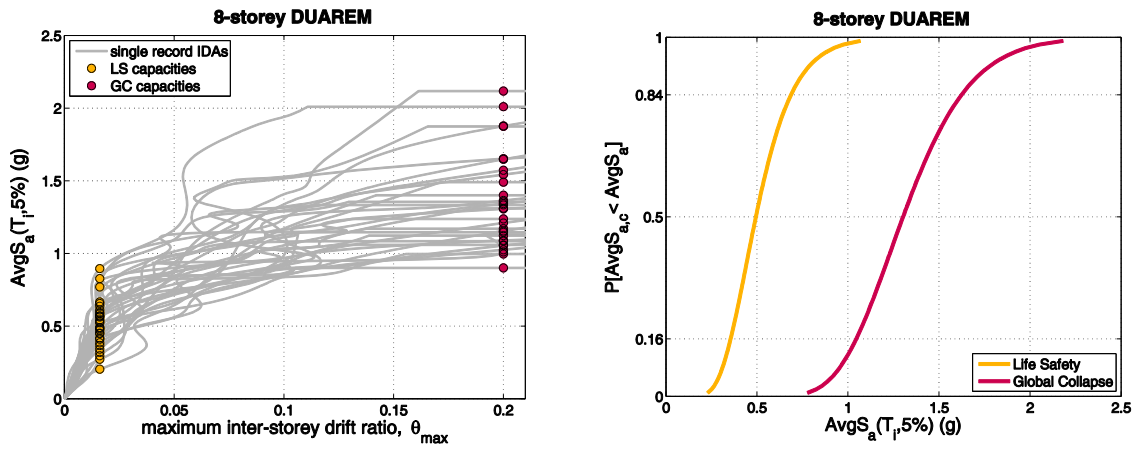
Table 8.1: Proposed acceptance criteria

	4-story		8-story	
Criteria	LS	GC	LS	GC
δ_{roof} (m)	0.124	∞	0.352	∞
θ_{max} (%)	0.91	∞	1.61	∞

8.3 Incremental Dynamic Analysis



a) b)
Fig. 8.6: 4-story structure: a) IDA and b) fragility curves



a) b)
Fig. 8.7: 8-story structure: a) IDA and b) fragility curves

8.4 q-factor verification

Table 8.2: Behaviour factor verification via the limit state mean annual frequency estimation

Site	Case study	Design q-factor	Limit State	$\lambda_x(DS)$ (‰)	λ_{DSlim} (‰)	Margin Ratio ($\lambda_{lim} / \lambda_x$)	Check	Next iteration q-factor
Athens	4-story	4	LS	1.925	2.107	1.095	✓	-
			GC	0.024	0.201	8.355		
	8-story	4	LS	1.099	2.107	1.917	✓	-
			GC	0.047	0.201	4.244		
Perugia	4-story	4	LS	1.443	2.107	1.460	✓	-
			GC	0.009	0.201	22.460		
	8-story	4	LS	0.951	2.107	2.216	✓	-
			GC	0.025	0.201	8.204		
Focsani	4-story	4	LS	2.559	2.107	0.823	✗	3.7
			GC	0.000	0.201	4225.83		
	8-story	4	LS	0.597	2.107	3.527	✓	-
			GC	0.000	0.201	1058.32		

9 SPSW thin-walled steel panels

9.1 Modelling

A nonlinear model is developed in OpenSees (Fig. 9.2b) to facilitate Incremental Dynamic Analysis for the case studies considered (Fig. 9.1). A simplified methodology for modelling the shear panels is used. In particular, the shear panels are idealised by 10 inclined tension pin-supported strip members, oriented in the same direction as the principal tensile stresses in the panel. Fig. 9.2a shows the strip model representation of a typical shear panel. The strips are modelled as double pinned beam elements and a trilinear backbone is used to capture the effect of the axial plastic hinge that is expected to form in the middle of the element. For the purpose of nonlinear dynamic analysis, the frame is modelled in the same manner as described above, only in this case 10 additional tension-only strips, mirrored about the vertical axis, are used to capture the cyclic loading effect (Fig. 9.2b). Nonlinear moment-rotation plastic hinges are assigned at the ends of MRF beams and columns, while a leaning column is used to account for the gravitational loads from the remaining half of structure that were not considered in the model.

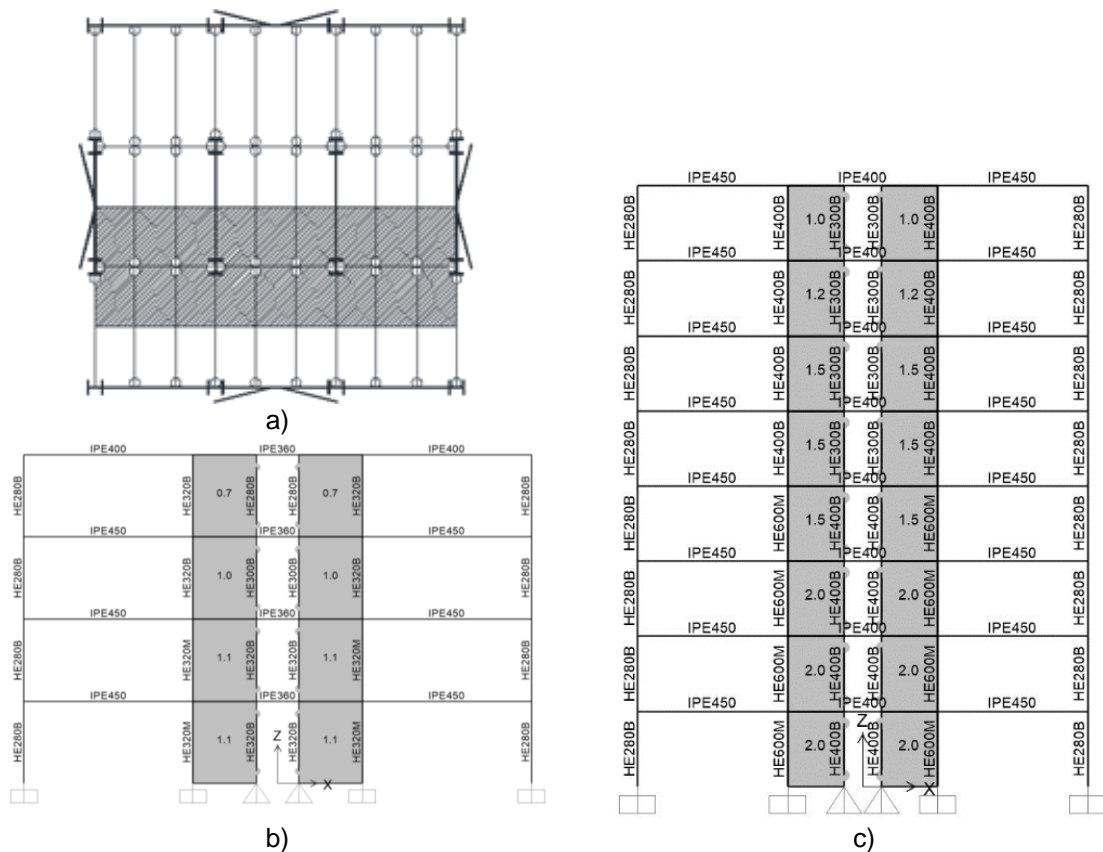


Fig. 9.1: Case-study building frames: a) Plan view, b) 4-story and c) 8-story

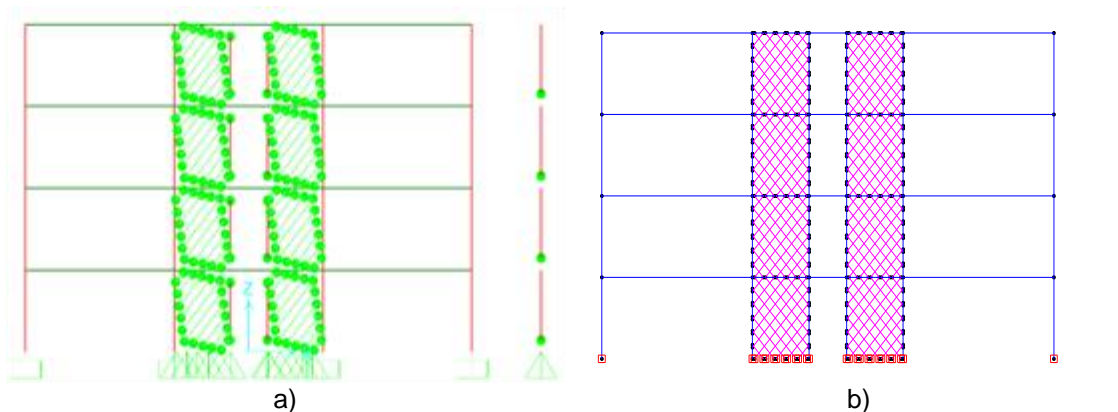


Fig. 9.2: 4-story numerical models: a) SAP2000 and b) OpenSees

9.2 Static Pushover Analysis

The OpenSees models are compared against existing SAP2000 models that were used for the design of these structures (Fig. 9.2a). Fig. 9.3 and Fig. 9.4 present a comparison between the deformed shapes of the three models, while Fig. 9.5 their respective (1st-mode load pattern) pushover curves, where P-delta effects are taken into account. Two capacity points representing the significant damage (LS) and global collapse (GC) limit states are also provided in Table 9.1. The aforementioned capacity points have been estimated by capturing failure on an element basis.

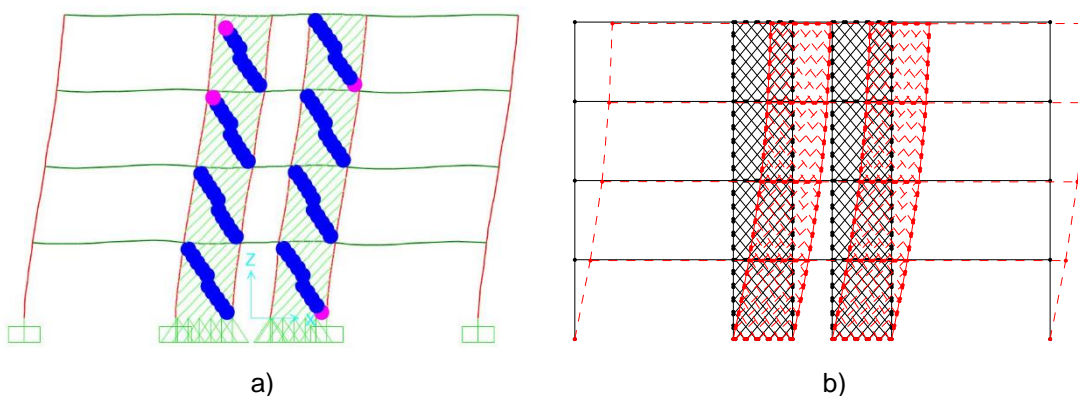
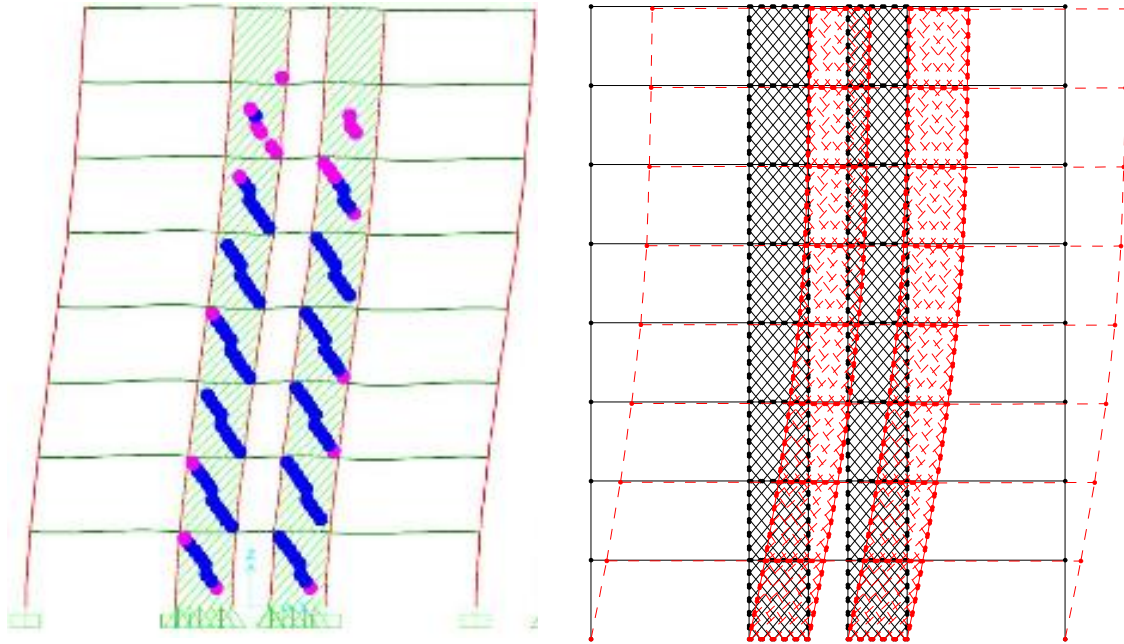
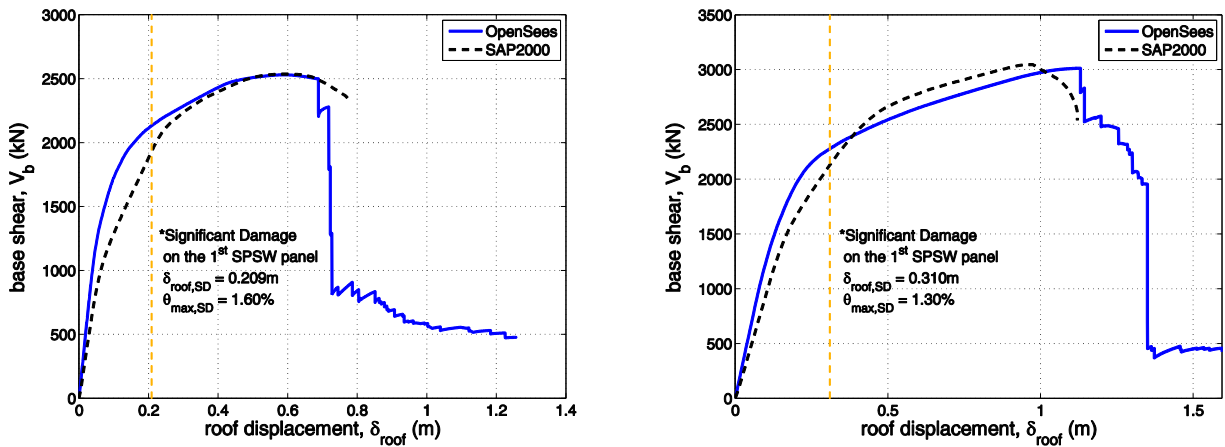


Fig. 9.3: 4-story model deflected shape: a) SAP2000 and b) OpenSees



a) b)
Fig. 9.4: 8-story model deflected shape: a) SAP2000 and b) OpenSees



a) b)
Fig. 9.5: OpenSees versus SAP2000 pushover curves: a) 4-story and b) 8-story structure

Table 9.1: Proposed acceptance criteria

Criteria	4-story		8-story	
	LS	GC	LS	GC
δ_{roof} (m)	0.209	∞	0.310	∞
θ_{max}	1.6	∞	1.3	∞

9.3 Incremental Dynamic Analysis

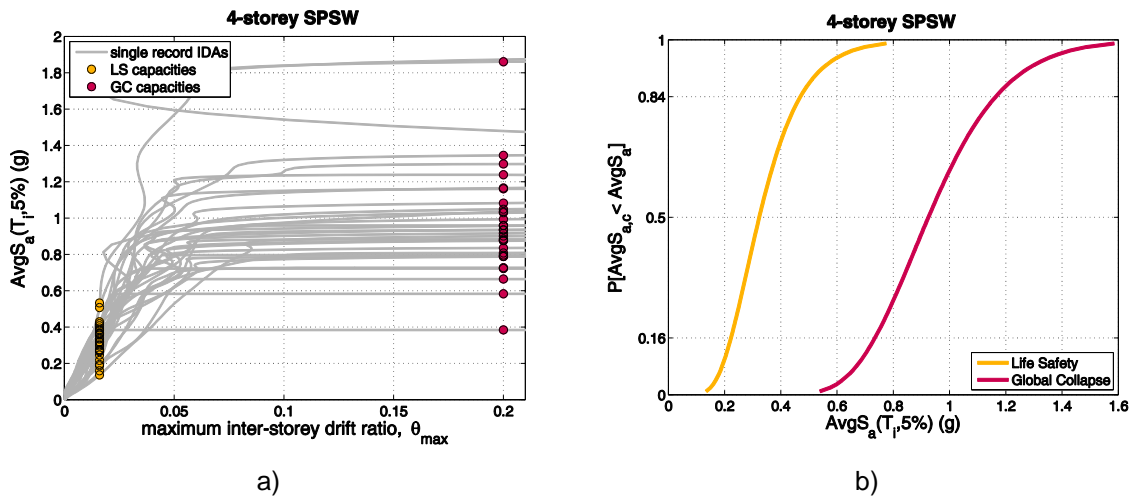


Fig. 9.6: 4-story structure: a) IDA and b) fragility curves

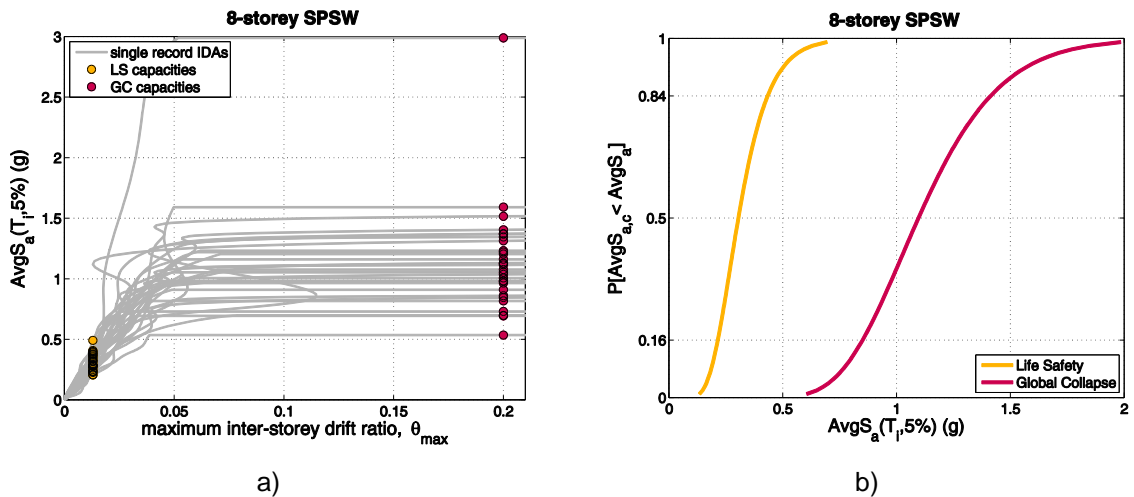


Fig. 9.7: 8-story structure: a) IDA and b) fragility curves

9.4 q-factor verification

Table 9.2: Behaviour factor verification via the limit state mean annual frequency estimation

Site	Case study	Design q-factor	Limit State	$\lambda_x(DS)$ (‰)	λ_{DSlim} (‰)	Margin Ratio ($\lambda_{lim} / \lambda_x$)	Check	Next iteration q-factor	
Athens	4-story	5	LS	3.386	2.107	0.622	✗	4.0	
			GC	0.194	0.201	1.037			
	8-story	5	LS	3.436	2.107	0.613	✗		
			GC	0.103	0.201	1.948			
Perugia	4-story	5	LS	3.190	2.107	0.660	✗	4.0	
			GC	0.119	0.201	1.688			
	8-story	5	LS	3.583	2.107	0.588	✗		3.8
			GC	0.065	0.201	3.093			
Focsani	4-story	5	LS	4.317	2.107	0.488	✗	3.8	
			GC	0.008	0.201	23.650			
	8-story	5	LS	5.217	2.107	0.404	✗		3.6
			GC	0.003	0.201	66.858			

10 CBF-MB Concentrically-braced frames with modified sections

10.1 Modelling

A nonlinear model is developed in OpenSees (Fig. 10.1b) to facilitate Incremental Dynamic Analysis for the case studies considered. The model consists of lumped plasticity elements for the members that are expected to undergo excessive deformations in the nonlinear range of the system; that primarily includes the modified braces, the splitting beams and the columns. Axial force-displacement plastic “hinges” are considered at the middle of the modified braces, with their properties being determined from calibration on experimental results and analytic investigations, while the non-dissipative elements are given hinge properties calculated according to the provisions of relevant codes (e.g. FEMA-356 [2]).

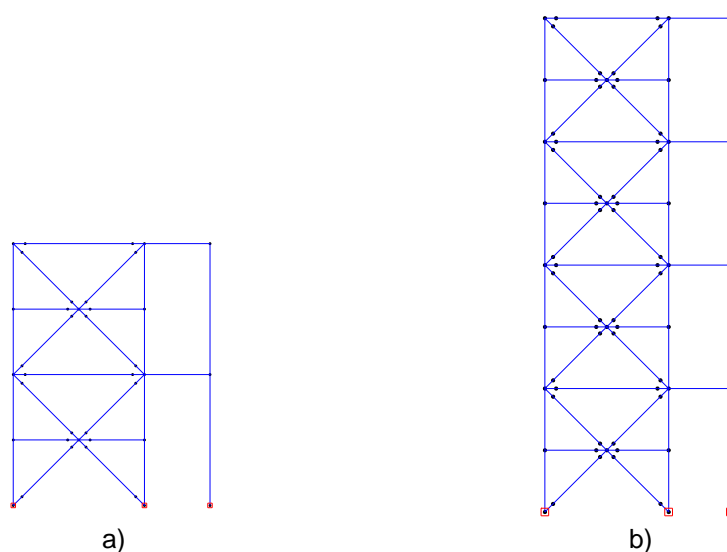


Fig. 10.1: OpenSees models: a) 2-storey and b) 4-storey

10.2 Static Pushover Analysis

The OpenSees models are compared against existing SAP2000 models that were used for the design of these structures (Fig. 10.1). Fig. 10.2 presents a comparison between the deformed shapes of the two models, while Fig. 10.3 their respective (1st-mode load pattern) pushover curves, where P-delta effects are taken into account. Two capacity points representing the significant damage (LS) and global collapse (GC) limit states are also provided in Table 10.1. The aforementioned capacity points have been estimated by capturing failure on an element basis.

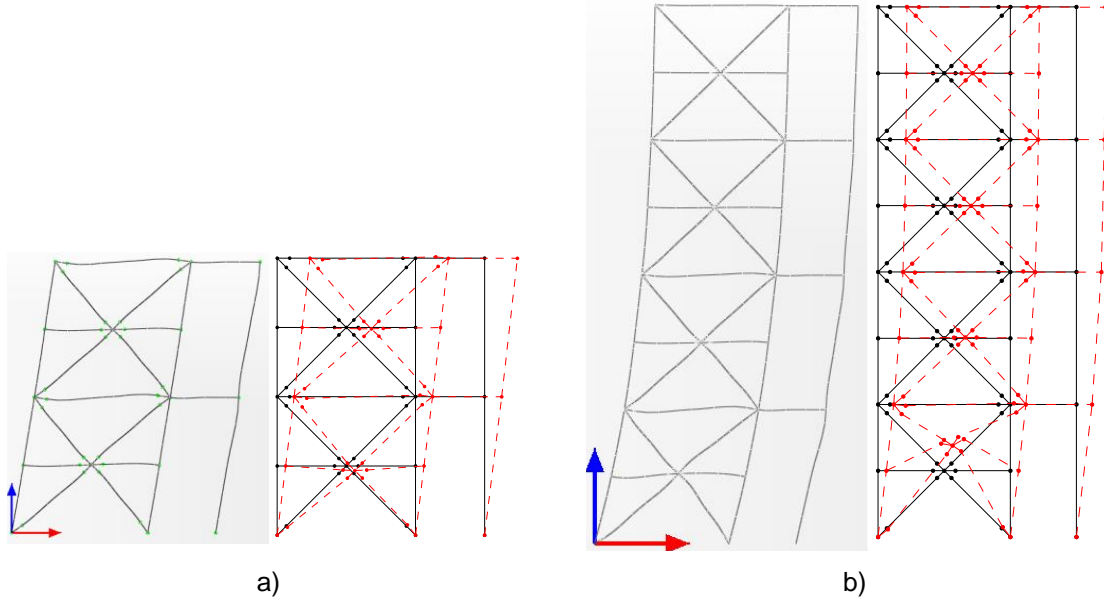


Fig. 10.2: Deflected shapes from SAP2000 and OpenSees: a) 2-storey and b) 4-storey

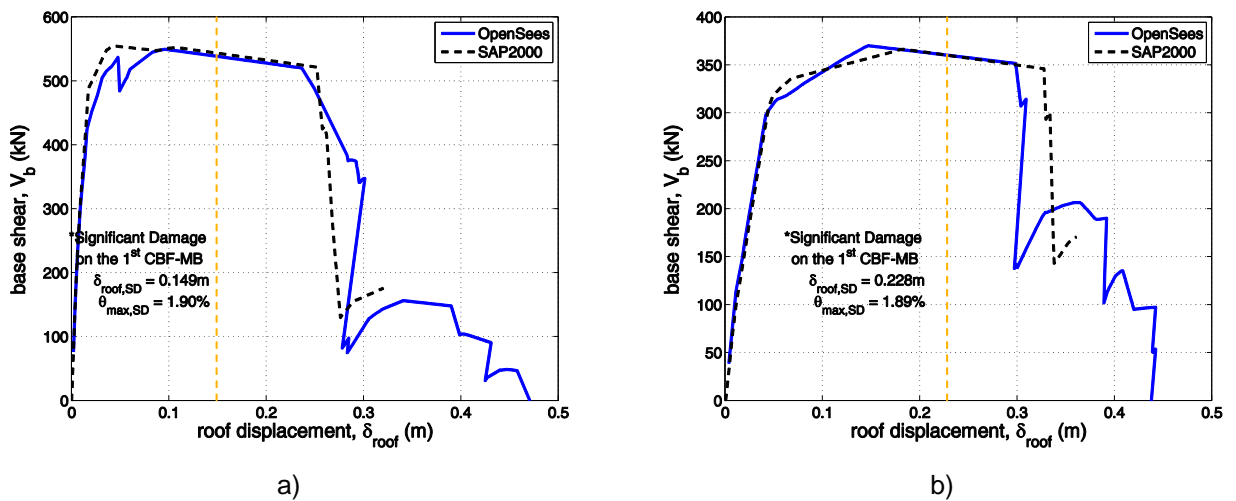


Fig. 10.3: OpenSees versus SAP2000 pushover curves: a) 2-story and b) 4-story structure

Table 10.1: Proposed acceptance criteria

Criteria	2-story		4-story	
	LS	GC	LS	GC
$\bar{\delta}_{roof}$ (m)	0.149	∞	0.228	∞
θ_{max} (%)	1.90	∞	1.89	∞

10.3 Incremental Dynamic Analysis

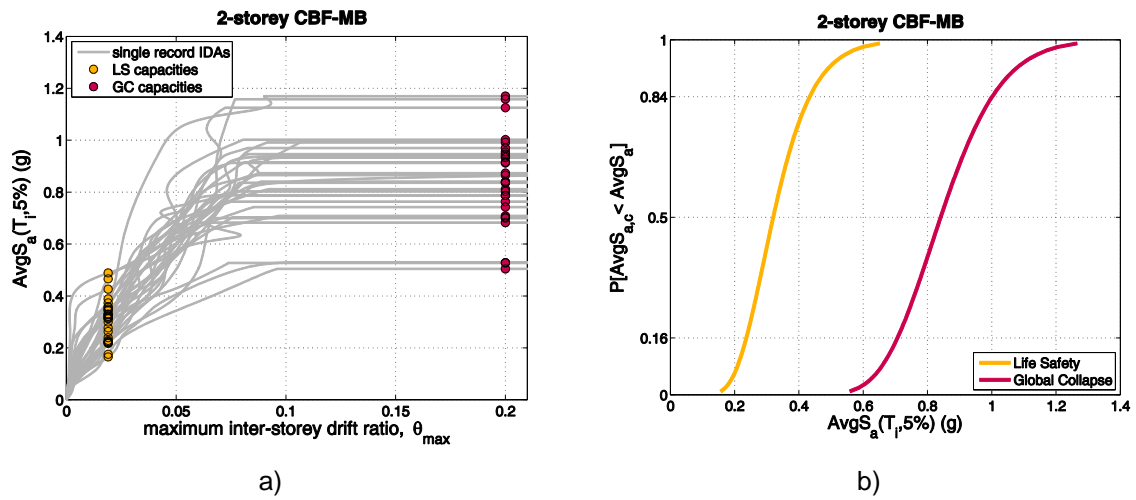


Fig. 10.4: 2-story structure: a) IDA and b) fragility curves

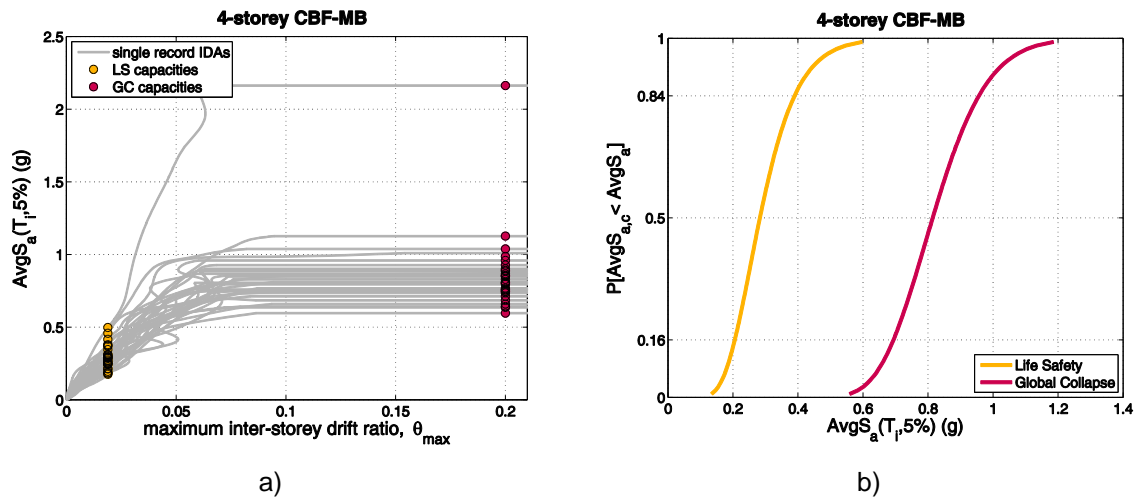


Fig. 10.5: 4-story structure: a) IDA and b) fragility curves

10.4 q-factor verification

Table 10.2: Behaviour factor verification via the limit state mean annual frequency estimation

Site	Case study	Design q-factor	Limit State	$\lambda_x(DS)$ (‰)	λ_{DSlim} (‰)	Margin Ratio ($\lambda_{lim} / \lambda_x$)	Check	Next iteration q-factor
Athens	2-story	5	LS	2.589	2.107	0.814	✗	4.5
			GC	0.200	0.201	1.004		
	4-story	5	LS	4.137	2.107	0.509	✗	3.6
			GC	0.260	0.201	0.773		
Perugia	2-story	5	LS	1.978	2.107	1.065	✓	-
			GC	0.102	0.201	1.970		
	4-story	5	LS	3.906	2.107	0.540	✗	3.7
			GC	0.161	0.201	1.251		
Focsani	2-story	5	LS	3.433	2.107	0.614	✗	4.2
			GC	0.009	0.201	21.445		
	4-story	5	LS	5.506	2.107	0.383	✗	3.6
			GC	0.010	0.201	19.862		

11 Concluding remarks

The assessment approach has in some cases verified the researchers' estimate of the q -factor, while in other cases it has rejected the trial q value. This does not necessarily mean that the q tested was erroneous. The proposed approach is not only a test for q , but also of the design methodology itself, the availability of adequate experimental results to accurately determine the behaviour of the sacrificial (or "dissipative") elements and the nonlinear modelling approach adopted. It is often the case that due to the conservative estimation of element ductility that researchers tend to self-impose, some lateral-load resisting systems may be penalized in terms of q . This should not be considered a bug but rather a useful feature of the procedure showcased. As more experience is gained and confidence grows in any given system, less conservative strength and ductility parameters can be adopted, allowing larger values for q .

References

1. Vamvatsikos D, Bakalis K, Kohrangi M, Thanopoulos P, Vayas I, Castiglioni C, Kanyilmaz A, *et al.* *Recommended procedure for EN1998-compatible behaviour factor evaluation of new structural systems*. Technical Report D2.1, INNOSEIS Consortium, Athens. <http://innoseis.ntua.gr/deliverables.php?deliverable=reports>, 2017.
2. FEMA. *Prestandard and Commentary for The Seismic Rehabilitation of Buildings*. FEMA-356, Prepared by the Building Seismic Safety Council for the Federal Emergency Management Agency, Washington, D.C., 2000.

List of Figures

Fig. 2.1: OpenSees numerical models: a) 2-story and b) 4-story.....	2
Fig. 2.2: Deflected shape: a) 2-story and b) 4-story.....	2
Fig. 2.3: OpenSees pushover curves: a) 2-story and b) 4-story structure	3
Fig. 2.4: 2-story structure: a) IDA and b) fragility curves.....	4
Fig. 2.5: 4-story structure: a) IDA and b) fragility curves.....	4
Fig. 3.1: Case studies: a) 2-story and b) 4-story.....	5
Fig. 3.2: Pushover curves: a) 2-story and b) 4-story structure	5
Fig. 4.1: OpenSees numerical models: a) 5-story and b) 10-story.....	6
Fig. 4.2: Deflected shape: a) 5-story and b) 10-story.....	7
Fig. 4.3: OpenSees pushover curves: a) 5-story and b) 10-story structure	7
Fig. 4.4: 5-story structure: a) IDA and b) fragility curves.....	8
Fig. 4.5: 10-story structure: a) IDA and b) fragility curves.....	8
Fig. 5.1: Case-study building frames: a) Plan view, b) 2-story and c) 4-story.....	9
Fig. 5.2: 4-story numerical models: a) SAP2000 and b) Opensees	10
Fig. 5.3: 2-story model deflected shape: a) SAP2000 and b) OpenSees	10
Fig. 5.4: 4-story model deflected shape: a) SAP2000 and b) OpenSees	10
Fig. 5.5: OpenSees versus SAP2000 pushover curves: a) 2-story and b) 4-story structure.....	11
Fig. 5.6: 2-story structure: a) IDA and b) fragility curves.....	11
Fig. 5.7: 4-story structure: a) IDA and b) fragility curves.....	12
Fig. 6.1: Distribution of assigned bolted beam splices.....	13
Fig. 6.2: OpenSees numerical models: a) 2-story, b) 4-story and c) 8-story.....	14
Fig. 6.3: 2-story model deflected shape: a) SAP2000 and b) OpenSees	14
Fig. 6.4: 4-story model deflected shape: a) SAP2000 and b) OpenSees	14
Fig. 6.5: 8-story model deflected shape: a) SAP2000 and b) OpenSees	15
Fig. 6.6: OpenSees versus SAP2000 pushover curves: a) 2-story, b) 4-story and c) 8- story.....	15
Fig. 6.7: 2-story structure: a) IDA and b) fragility curves.....	16
Fig. 6.8: 4-story structure: a) IDA and b) fragility curves.....	16
Fig. 6.9: 8-story structure: a) IDA and b) fragility curves.....	16
Fig. 7.1: OpenSees numerical models: a) 2-story, b) 4-story and c) 8-story.....	18
Fig. 7.2: Side view of the modelled building: (a) internal frames and (b) external frames. The reinforced beam zones are highlighted in orange in which the marks that represent the welded FUSEIS can be observed.	19
Fig. 7.3: Plan view of the modelled building (the reinforced beam zones and the welded FUSEIS are not represented).....	19
Fig. 7.4: Schematic representation of the composite slab	19
Fig. 7.5: OpenSees models: a) 2-story and b) 4-story	20
Fig. 7.6: 8-story model deflected shape: a) SAP2000 and b) OpenSees	20
Fig. 7.7: OpenSees versus SAP2000 pushover curves: a) 2-story, b) 4-story and c) 8- story.....	21
Fig. 7.8: 2-story structure: a) IDA and b) fragility curves.....	22
Fig. 7.9: 4-story structure: a) IDA and b) fragility curves.....	22
Fig. 7.10: 8-story structure: a) IDA and b) fragility curves.....	22
Fig. 8.1: 4-story numerical models: a) SAP2000 and b) Opensees	24
Fig. 8.2: Case-study building frames: a) Plan view, b) 4-story and c) 8-story.....	24
Fig. 8.3: 4-story model deflected shape: a) SAP2000 and b) OpenSees	25

Fig. 8.4: 8-story model deflected shape: a) SAP2000 and b) OpenSees 25

Fig. 8.5: OpenSees versus SAP2000 pushover curves: a) 4-story and b) 8-story structure..... 25

Fig. 8.6: 4-story structure: a) IDA and b) fragility curves..... 26

Fig. 8.7: 8-story structure: a) IDA and b) fragility curves..... 26

Fig. 9.1: Case-study building frames: a) Plan view, b) 4-story and c) 8-story 28

Fig. 9.2: 4-story numerical models: a) SAP2000 and b) Opensees 29

Fig. 9.3: 4-story model deflected shape: a) SAP2000 and b) OpenSees 29

Fig. 9.4: 8-story model deflected shape: a) SAP2000 and b) OpenSees 30

Fig. 9.5: OpenSees versus SAP2000 pushover curves: a) 4-story and b) 8-story structure..... 30

Fig. 9.6: 4-story structure: a) IDA and b) fragility curves..... 31

Fig. 9.7: 8-story structure: a) IDA and b) fragility curves..... 31

Fig. 10.1: OpenSees models: a) 2-storey and b) 4-storey 32

Fig. 10.2: Deflected shapes from SAP2000 and OpenSees: a) 2-storey and b) 4-storey..... 33

Fig. 10.3: OpenSees versus SAP2000 pushover curves: a) 2-story and b) 4-story structure..... 33

Fig. 10.4: 2-story structure: a) IDA and b) fragility curves..... 34

Fig. 10.5: 4-story structure: a) IDA and b) fragility curves..... 34

List of Tables

Table 2.1: Proposed acceptance criteria	3
Table 2.2: Behaviour factor verification via the limit state mean annual frequency estimation	4
Table 4.1: Proposed acceptance criteria	7
Table 4.2: Behaviour factor verification via the limit state mean annual frequency estimation	8
Table 5.1: Proposed acceptance criteria	11
Table 5.2: Behaviour factor verification via the limit state mean annual frequency estimation	12
Table 6.1: Proposed acceptance criteria	15
Table 6.2: Behaviour factor verification via the limit state mean annual frequency estimation	17
Table 7.1: Proposed acceptance criteria	21
Table 7.2: Behaviour factor verification via the limit state mean annual frequency estimation	23
Table 8.1: Proposed acceptance criteria	26
Table 8.2: Behaviour factor verification via the limit state mean annual frequency estimation	27
Table 9.1: Proposed acceptance criteria	30
Table 9.2: Behaviour factor verification via the limit state mean annual frequency estimation	31
Table 10.1: Proposed acceptance criteria	33
Table 10.2: Behaviour factor verification via the limit state mean annual frequency estimation	34